

Electronic and Steric Effects in the Insertion of Alkynes into an Iridium(III) Hydride

Xingwei Li, Tiffany Vogel, Christopher D. Incarvito, and Robert H. Crabtree*

Department of Chemistry, Yale University, 225 Prospect Street, New Haven, Connecticut 06520

Received September 18, 2004

Insertion of a variety of alkynes into the Ir–H bond of *trans*-[IrH(PPh₃)₂](C(Ph)=CHC(O)Me)(acetone)]⁺ (**1**) follows three different routes depending on the alkyne structures. For relatively electron-rich alkynes (PhC≡CH, PhCH₂C≡CH, and *p*-OMeC₆H₄C≡CH), double insertion occurs stepwise, each alkyne undergoing rearrangement to a vinylidene intermediate independently to afford an iridium(III) η^2 -butadienyl. In the first alkyne insertion, deuterium labeling and crossover experiments confirm that the alkyne to vinylidene rearrangement is intraligand. Both a vinyl and a vinylidene intermediate were trapped and isolated during this first insertion. In the second alkyne insertion, a C–H agostic intermediate was isolated. Electron-poor alkynes (*p*-CF₃C₆H₄C≡CH and *p*-NO₂C₆H₄C≡CH) also undergo double insertion into **1**, but deuterium labeling experiments using *p*-CF₃C₆H₄C≡CD indicate reversible C(sp)–H oxidative addition. Insertion of highly polarized alkynes [R₁C≡CC(O)–R₂] to **1** occurs only once and involves no vinylidene intermediates even when R₁ = H. The regio- and stereochemistry in this case are mainly controlled by the steric effects of R₁. In this series, rare *cis*-(PPh₃)₂ intermediates were isolated for HC≡CC(O)R (R = Me or OMe). X-ray crystal structures of representative products are reported.

1. Introduction

Alkyne insertion into metal hydrides (M–H) is a fundamental step in many homogeneous catalytic reactions such as alkyne hydrogenation, hydrosilylation, and oligomerization.¹ Insertion can be followed by stoichiometric or catalytic C–C bond forming steps for organic synthetic applications such as the synthesis of a variety of polyenes.^{2–4} Despite its apparent simplicity, at least three possible mechanisms have previously been proposed for the insertion of alkynes into M–H to give vinyls (Scheme 1). In path (a),⁵ the direct insertion of an alkyne into the M–H bond via a four-centered transition state affords the *syn*-insertion product; this may then isomerize to the apparent *anti*-insertion product via proposed η^2 -vinyl intermediates.⁶ In path (b), the RC≡CH first rearranges to a vinylidene ligand

by a concerted intraligand 1,2-hydrogen shift, which was proposed before based on theoretical studies,^{1a,4,7} followed by migratory insertion of the vinylidene into the M–H bond to give a vinyl.⁸ Path (c) involves a C(sp)–H oxidative addition to the metal to give a metal dihydride or a dihydrogen intermediate,⁹ followed by a unimolecular 1,3-hydrogen shift or a bimolecular proton shift^{9c} from the metal to the ligand to form a vinylidene, which

(1) (a) Oliván, M.; Clot, E.; Eisenstein, O.; Caulton, K. G. *Organometallics* **1998**, *17*, 3091 and references cited there. (b) Otsuka, S.; Nakamura, A. *Adv. Organomet. Chem.* **1974**, *14*, 245. (c) Dash, A. K.; Wang, J.-Q.; Eisen, M. S. *Organometallics* **1999**, *18*, 4724. (d) Bianchini, C.; Innocenti, P.; Meli, A.; Peruzzini, M.; Zanobini, F.; Zanello, P. *Organometallics* **1990**, *9*, 2514.

(2) (a) Chin, C. S.; Kim, M.; Lee, H.; Noh, S.; Ok, K. M. *Organometallics* **2002**, *21*, 4785. (b) Esteruelas, M. A.; Gracia-Yebra, C.; Oliván, M.; Onate, E.; Tajada, M. A. *Organometallics* **2000**, *19*, 5098. (c) Deng, M.; Leong, W. K. *Organometallics* **2002**, *21*, 1221. (d) Sola, E.; Torres, O.; Plou, P.; Oro, L. A. *Organometallics* **2003**, *22*, 5406. (e) Slugovc, C.; Mereiter, K.; Zobetz, E.; Schmid, R.; Kirchner, K. *Organometallics* **1996**, *15*, 5275. (f) Johnson, J. R.; Cuny, G. D.; Buchwald, S. L. *Angew. Chem., Int. Ed. Engl.* **1995**, *34*, 1760. (g) Esteruelas, M. A.; Herrero, J.; Lopez, A. M.; Oliván, M. *Organometallics* **2001**, *20*, 3202.

(3) (a) Kishimoto, Y.; Eckerle, P.; Miyatake, T.; Kainosho, M.; Ono, A.; Ikariya, T.; Noyori, R. *J. Am. Chem. Soc.* **1999**, *121*, 12035. (b) Burrows, A. D.; Green, M.; Jeffery, J. C.; Lynam, J. M.; Mahon, M. F. *Angew. Chem., Int. Ed.* **1999**, *38*, 3043. (c) Chin, C. S.; Lee, H.; Park, H.; Kim, M. *Organometallics* **2002**, *21*, 3889. (d) Selnau, H. E.; Merola, J. S. *J. Am. Chem. Soc.* **1991**, *113*, 4008.

(4) Li, X.; Incarvito, C. D.; Crabtree, R. H. *J. Am. Chem. Soc.* **2003**, *125*, 3698.

(5) For regio- and stereochemistry of alkyne insertion, see: (a) Navarro, J.; Sola, E.; Martin, M.; Dobrinovitch, I. T.; Lahoz, F. J.; Oro, L. A. *Organometallics* **2004**, *23*, 1908. (b) Frohnapfel, D. S.; White, P. S.; Templeton, J. L. *Organometallics* **2000**, *19*, 1497. (c) Selmecky, A. D.; Jones, W. D. *Inorg. Chim. Acta* **2000**, *300–302*, 138. (d) Herberich, G. E.; Barriage, W. *Organometallics* **1987**, *6*, 1924. (e) Bassetti, M.; Casellato, P.; Gamasa, M. P.; Gimeno, J.; Gonzalez-Bernardo, C.; Martin-vaca, B. *Organometallics* **1997**, *15*, 5470. (f) Gao, Y.; Jennings, M. C.; Puddephatt, R. L. *Dalton Trans.* **2003**, 261. (g) Bassetti, M.; Marini, S.; Diaz, J.; Gamasa, M. P.; Gimeno, J.; Rodriguez-Alvarez, Y.; Garcia-Granda, S. *Organometallics* **2002**, *21*, 4815.

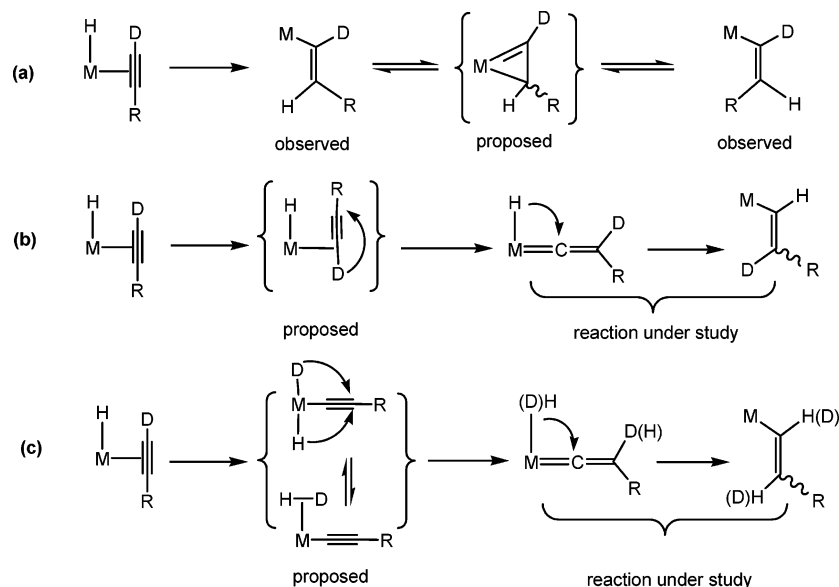
(6) (a) Chung, L. W.; Wu, Y.-D.; Trost, B. M.; Ball, Z. T. *J. Am. Chem. Soc.* **2003**, *125*, 11578. (b) Crabtree, R. H. *New J. Chem.* **2003**, *27*, 771. (c) Tanke, R. S.; Crabtree, R. H. *J. Am. Chem. Soc.* **1990**, *112*, 7984. (d) Ojima, I.; Clos, N.; Donovan, R. J.; Ingallina, P. *Organometallics* **1990**, *9*, 3127. (e) Frohnapfel, D. S.; Templeton, J. L. *Coord. Chem. Rev.* **2000**, *206*, 199.

(7) (a) Silvestre, J.; Hoffmann, R. *Helv. Chim. Acta* **1985**, *68*, 1461. (b) Wakatsuki, Y.; Koga, N.; Yamazaki, H.; Morokuma, K. *J. Am. Chem. Soc.* **1994**, *116*, 8105. (c) Cadierno, V.; Gamasa, M. P.; Gimeno, J.; Pérez-Carreño, E.; Garcia-Granda, S. *Organometallics* **1999**, *18*, 2821. (d) Akita, M.; Ishii, N.; Takabuchi, A.; Tanaka, M.; Moro-oka, Y. *Organometallics* **1994**, *13*, 258. (e) De Angelis, F.; Sgamellotti, A.; Re, N. *Organometallics* **2002**, *21*, 2715.

(8) (a) Esteruelas, M. A.; Oro, L. A.; Valero, C. *Organometallics* **1995**, *14*, 3596. (b) Buil, M. L.; Esteruelas, M. A. *Organometallics* **1999**, *18*, 1798.

(9) (a) Li, X.; Appelhans, L. N.; Faller, J. W.; Crabtree, R. H. *Organometallics* **2004**, *23*, 3378. (b) De los Ríos, I.; Tenorio, M. J.; Puerta, M. C.; Valerga, P. *J. Am. Chem. Soc.* **1997**, *119*, 6529. (c) Wakatsuki, Y.; Koga, N.; Werner, H.; Morokuma, K. *J. Am. Chem. Soc.* **1997**, *119*, 360. (d) Windmüller, B.; Wolf, J.; Werner, H. *J. Organomet. Chem.* **1995**, *502*, 147. (e) Garcia Alonso, F. J.; Hoehn, A.; Wolf, J.; Otto, H.; Werner, H. *Angew. Chem.* **1985**, *97*, 401. (f) Torkelson, J. R.; McDonald, R.; Cowie, M. *Organometallics* **1999**, *18*, 4134.

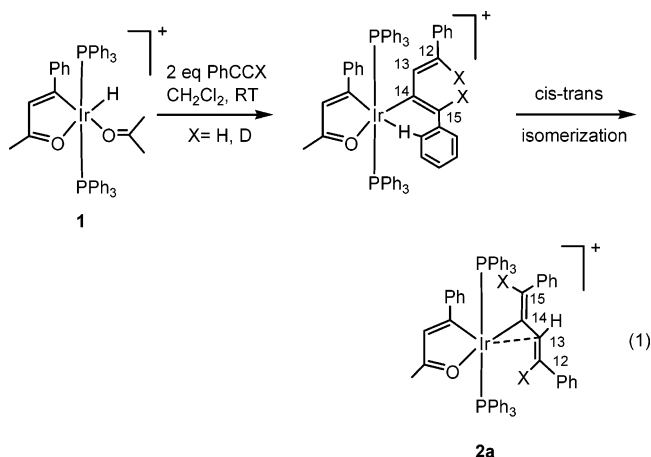
Scheme 1



then might undergo migratory insertion to yield a vinyl as in path (b). In contrast to path (b), however, the hydrides in path (c) are not spectators in the vinylidene formation step. In both path (b) and (c), the well-known alkyne to vinylidene rearrangement¹⁰ is involved. Fully authenticated examples of alkyne insertion through paths (b) and (c) are rare because they have been mostly proposed theoretically rather than shown experimentally. This multiplicity of pathways makes the outcome in any specific case hard to determine or predict.

Insertion of an alkyne into a metal hydride usually requires a cis vacant site to accommodate the alkyne. Since the insertion process would regenerate this site, double or even multiple alkyne insertion that forms C–C bonds should be possible in principle. These are not very common, however, no doubt due to the fact that the second alkyne insertion into the first-formed vinyl is expected to be slower than the first insertion into hydride. The second alkyne insertion is normally much less favorable probably as a result of the following effects: (1) the steric hindrance is greater; (2) coordination of some pendant functional groups in the resultant vinyl may occur,^{11–14} (3) there may be coupling between the vinyl ligand and other ligands,^{9a,15} and occasionally (4) stable coordinatively saturated η^2 -vinyl complexes can be formed.¹⁶ Despite their rarity, double or even multiple insertion of alkynes into metal hydrides has occasionally been reported.^{2b,3,4}

We have briefly reported the double insertion of unactivated alkynes into the iridium hydride **1** to afford a rare Ir(III) η^2 -butadienyl.⁴ As reported in full here, deuterium labeling and crossover experiments indicate that each alkyne undergoes independent rearrangement to give a vinylidene (eq 1). The first vinylidene inserts into the hydride to form a vinyl intermediate, into which the second vinylidene inserts to give a proposed intermediate, observed in one case, stabilized by a C–H agostic bond. This agostic intermediate can then rearrange to yield the observed Ir(III) η^2 -butadienyl product. In this paper we look in full at the intermediates involved in the double insertion and find that electronic and steric effects of the alkynes can change the pathway of the insertion into the same Ir(III) hydride.



2. Results and Discussion

2.1. Alkyne Double Insertion Involving Intraligand Alkyne to Vinylidene Rearrangement (path (b), Scheme 1). Addition of 2 equiv of the relatively electron-rich terminal alkynes ($\text{RC}\equiv\text{CH}$, $\text{R} = \text{Ph}$, PhCH_2 , and $p\text{-C}_6\text{H}_4\text{OMe}$) to **1** in acetone or CH_2Cl_2 caused an immediate color change from yellow to orange; yellow precipitates were obtained with Et_2O . The products were characterized as η^2 -butadienyls **2a–c** ($\text{X} = \text{H}$) on the basis of ^1H , ^{31}P , and ^{13}C NMR spectroscopy, X-ray

(10) Reviews: (a) Bruneau, C.; Dixneuf, P. H. *Acc. Chem. Res.* **1999**, *32*, 311. (b) Bruce, M. I. *Chem. Rev.* **1991**, *91*, 197.

(11) van der Zeijden, A. A. H.; Bosch, H. W.; Berke, H. *Organometallics* **1992**, *11*, 563.

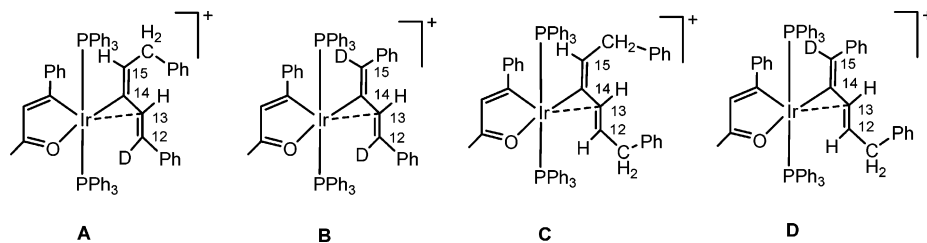
(12) Esteruelas, M. A.; García, M. P.; Martín, M.; Nürnberg, O.; Oro, L. A.; Werner, H. *J. Organomet. Chem.* **1994**, *466*, 249.

(13) (a) Atencio, R.; Bohanna, C.; Esteruelas, M. A.; Lahoz, F. J.; Oro, L. A. *J. Chem. Soc., Dalton Trans.* **1995**, 2171. (b) Echavarren, A. M.; Lopez, J.; Santos, A.; Romero, A.; Hermoso, J. A.; Vegas, A. *Organometallics* **1991**, *10*, 2371. (c) Werner, H.; Meyer, U.; Peters, K.; von Schnering, H. G. *Chem. Ber.* **1989**, *122*, 2097.

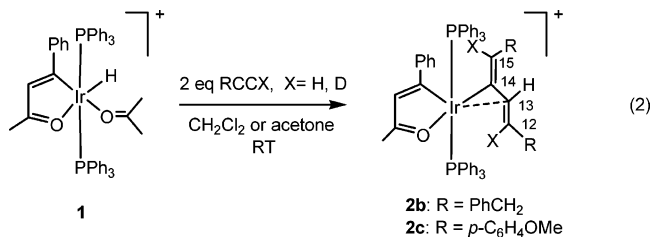
(14) (a) Albertin, G.; Antoniutti, S.; Bordignon, E. *J. Chem. Soc., Dalton Trans.* **1995**, 719. (b) Esteruelas, M. A.; Lahoz, F. J.; Oro, L. A.; Schluncken, C.; Valero, C.; Werner, H. *Organometallics* **1992**, *11*, 2034.

(15) Wen, T. B.; Zhou, Z. Y.; Jia, G. *Organometallics* **2003**, *22*, 4947.

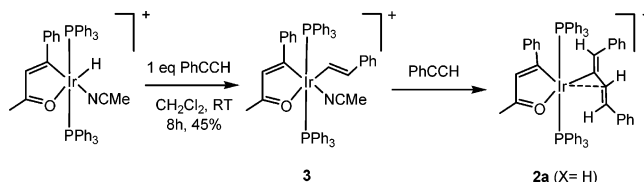
(16) (a) Stone, K. C.; Jamison, G. M.; White, P. S.; Templeton, J. L. *Organometallics* **2003**, *22*, 3083. (b) Frohnapfel, D. S.; White, P. S.; Templeton, J. L. *Organometallics* **2000**, *19*, 14797.

**Figure 1.**

crystallography (for **2a**, X = H), and elemental analysis (eqs 1, 2). Both ^1H and ^{13}C NMR spectroscopy indicate that two alkyne units have been incorporated. In particular, the $^{13}\text{C}\{^1\text{H}\}$ NMR spectrum shows a high-field singlet signal for C(sp²) [δ 100.3 (s) for **2a** (X = H); 99.4 (s) for **2b** (X = H), 96.5 (s) for **2c** (X = H)], assigned to C(13) on the basis of comparison with previous data.¹⁷ The ^1H NMR spectrum (acetone-*d*₆) shows two mutually trans-coupled HC=CH protons [H(12) and H(13); crystallographic numbering (see Figure 3) is used throughout, δ 6.42 (d, $^3J_{\text{HH}} = 16.2$ Hz) and 5.59 (d, $^3J_{\text{HH}} = 16.2$ Hz) for **2a** (X = H); 5.29 (dt, $^3J_{\text{HH}} = 15.2$ Hz) and 4.92 (d, $^3J_{\text{HH}} = 15.2$ Hz) for **2b** (X = H); 6.38 (d, $^3J_{\text{HH}} = 16.0$) and 5.32 (d, $^3J_{\text{HH}} = 16.0$ Hz) for **2c** (X = H)]. Assignment of H(12) and H(13) by C–H correlation spectroscopy showed that H(12) always resonates to higher field of H(13). This assignment is also confirmed by the additional coupling found between C(12) and its adjacent CH₂ group in **2b** (X = H). The $^{31}\text{P}\{^1\text{H}\}$ NMR spectra of **2a–c** show a singlet for each complex. The X-ray crystal structure of **2a** (X = H) confirmed the bihapticity of the η^2 -butadienyl group.⁴

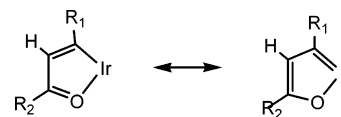


Deuterium labeling experiments show that R and D always stay attached to both C(12) and C(15), which used to be the C-2 positions of the alkyne unit (eqs 1, 2). A crossover experiment was performed using hydride **1** and a mixture of PhCH₂C≡CH and PhC≡CD. All four η^2 -butadienyl products (**A–D**, Figure 1) were obtained with a ratio of **A:B:C:D** = 1.00:1.56:0.76:0.73, based on ^{31}P and ^1H NMR analysis, where complex **B** is **2a** (X = D) and complex **C** is **2b** (X = H), whose ^1H NMR spectra are known. By comparison with the ^1H NMR spectra of the four products obtained from **1** and a mixture of PhC≡CH and PhCH₂C≡CH, the H(12) and H(15) signals associated with PhCH₂ or Ph in **A–D** can be separately distinguished and assigned. In particular, ^1H NMR signals for H(12) (δ 6.18) of **A**, H(12) (δ 6.42) and H(15) (δ 5.72) of **B**, and H(15) of **D** (δ 5.67) essentially disappear (<4% residual signal). Furthermore, the absence of any resonance signal between δ 3.0 and 6.0 in the ^2H NMR (76.77 MHz, 298 K, acetone-*d*₆) spectrum of the mixture confirmed the absence of any D-12 in **C**

Scheme 2

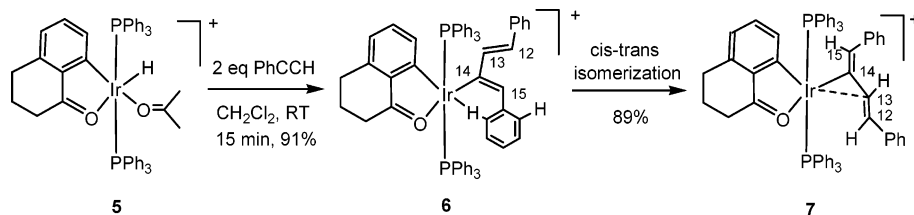
and **D** and D-15 in **A** and **C**. These results show that PhCH₂ and H are always attached to the same carbon in the four products, as are Ph and D, and there is no crossover between these two alkyne units.

These experiments suggest that eq 1 goes by initial alkyne insertion via path (b) in Scheme 1. No simple vinyl intermediate was obtained from **1** and 1 equiv of PhC≡CH in acetone, which gave only the double insertion product **2a** (X = H) (50% yield) and starting material **1**. The insertion of the second alkyne to lead to **2a** is therefore faster than that of the first. By moving to the acetonitrile adduct of **1**, however, the first vinyl intermediate can be successfully trapped (Scheme 2). Acetonitrile, more ligating than acetone, may inhibit the binding of the second alkyne. In this reaction, a mixture of the starting material, the simple vinyl complex **3**, and the double-insertion product **2a** (X = H) was detected in a ratio of 0.5:10:1 by ^1H and ^{31}P NMR spectroscopy (CD₂Cl₂, 25 °C, 8 h). The vinyl **3** was readily isolated owing to its greater solubility in diethyl ether and was fully characterized. The ^1H NMR spectrum of **3** (CD₂Cl₂) shows a characteristic low-field resonance of a triplet ($^3J_{\text{PH}} = 3.0$ Hz) of doublets ($^3J_{\text{HH}} = 16.4$ Hz) at δ 8.22, assigned to the α -H of the styrenyl group, while the β -H in this group resonates as a doublet ($^3J_{\text{HH}} = 16.4$ Hz) at δ 5.85. The coupling constant between these two protons clearly indicates a trans orientation on the C=C double bond. The $^{13}\text{C}\{^1\text{H}\}$ NMR spectrum of **3** shows a very low field triplet at δ 204.5 ($^2J_{\text{PC}} = 7.4$ Hz), assigned to the vinyl carbon of the iridacycle. This carbenoid chemical shift suggests that this iridacycle is essentially an iridafuran due to the presence of two resonance structures (Figure 2). Another triplet at δ 118.4 ($^2J_{\text{PC}} = 9.0$ Hz) is assigned to the α -carbon of the styrenyl group. The ^{13}C NMR spectrum confirmed the presence of a CH₃CN ligand (δ 3.2, CH₃; δ 121.8 CN). Addition of phenyl acetylene to a dichloromethane solution of **3** slowly but cleanly leads to the double insertion product **2a** (X = H), indicating that the vinyl complex **3** is indeed an intermediate in alkyne double insertion.

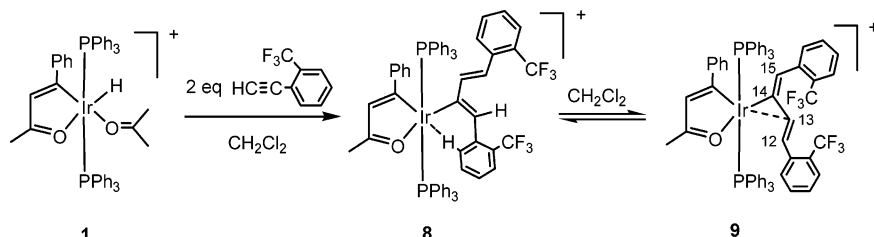
**Figure 2.**

(17) (a) Karl, J.; Erker, G.; Fröhlich, R. *J. Am. Chem. Soc.* **1997**, *119*, 11165. (b) Jia, G.; Lee, H. M.; Xia, H. P.; Williams, I. D. *Organometallics* **1996**, *15*, 5453.

Scheme 3

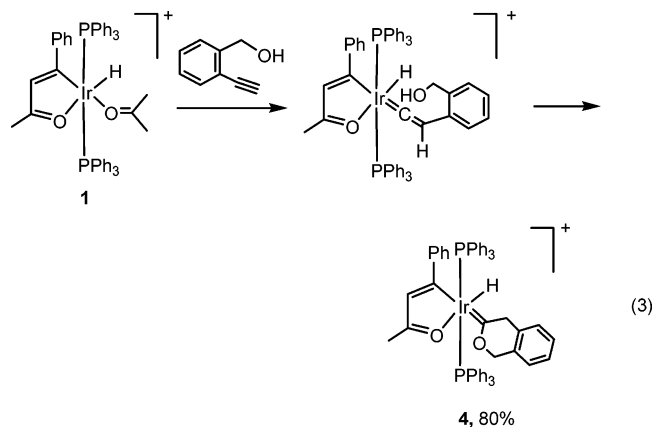


Scheme 4



Although deuterium labeling experiments with $\text{RC}\equiv\text{CD}$ ($\text{R} = \text{Ph}, \text{PhCH}_2$, and $o\text{-C}_6\text{H}_4\text{OMe}$) indicate we have an alkyne to vinylidene rearrangement, all attempts failed to observe the proposed vinylidene intermediate by ^1H NMR spectroscopy (acetone- d_6 , -30°C). The vinylidene ligand may be destabilized by being trans to the high trans-effect ligand (the iridafuran carbon).

Independent evidence for this vinylidene intermediate was obtained from trapping the vinylidene by nucleophilic attack of an $-\text{OH}$ group. In this reaction of a functionalized alkyne 2-ethynylbenzyl alcohol and hydride **1**, the iridium carbene hydride **4** was obtained (eq 3), which was fully characterized by ^1H , ^{13}C , and ^{31}P NMR spectroscopy. In particular, the $^{13}\text{C}\{^1\text{H}\}$ NMR spectrum (CD_2Cl_2) shows the Fischer carbene resonates as a triplet at δ 292.5 ($^2J_{\text{PC}} = 7.9$ Hz) and the two ring CH_2 groups at δ 79.4 (s) and 59.6 (s). In the ^1H NMR spectrum (CD_2Cl_2), the hydride resonates as a triplet at δ -20.96 ($^2J_{\text{PH}} = 14$ Hz) and the two CH_2 groups resonate at δ 4.53 (s, 2H) and 3.51 (s, 2H). Our proposed pathway (eq 3) goes by intramolecular trapping of the vinylidene by the pendant hydroxyl group to generate a stable, cyclic carbene.^{2a,18} The fact that **4** is the only product shows that this trapping is faster than the alternative vinylidene insertion into $\text{Ir}-\text{H}$ to yield a vinyl.⁸



The mechanism of the formation of the final η^2 -butadienyl complex from the simple vinyl, also studied

by deuterium labeling, involves a second alkyne to vinylidene rearrangement. Intermediates for this second insertion were studied by reaction of $\text{PhC}\equiv\text{CH}$ with **5**, an analogue of **1** (Scheme 3). This reaction rapidly (15 min, RT) afforded **6**, a C–H agostic complex, which was readily isolated. Reflux of a dichloromethane solution of **6** for 10 h afforded the η^2 -butadienyl **7** in high yield. Both **6** and **7** were fully characterized by NMR spectroscopy with confirmation of the C–H agostic product by X-ray crystallography.⁴ In the ^1H NMR spectrum (CD_2Cl_2) at room temperature, a characteristic broad singlet at δ 5.21 (2H) was assigned to the C–H agostic protons broadened by fluxionality caused by the rotation of the C–C(phenyl) bond. Upon cooling, this signal decoalesced to broad singlets at δ 3.80 and 6.54 at -75°C . In the $^{13}\text{C}\{^1\text{H}\}$ NMR spectrum of **6** at -80°C , decoalescence of signals for the agostic Ph ring at δ 107.2 (C-2', agostic), 126.6 (C-6'), 136.3 (C3'), and 130.3 (C5') was also confirmed by C–H correlation spectroscopy. $\text{C}(\text{sp}^3)\text{-H}$ agostic complexes are well-known, but $\text{C}(\text{sp}^2)\text{-H}$ agostic ones are somewhat rarer.^{2a,19}

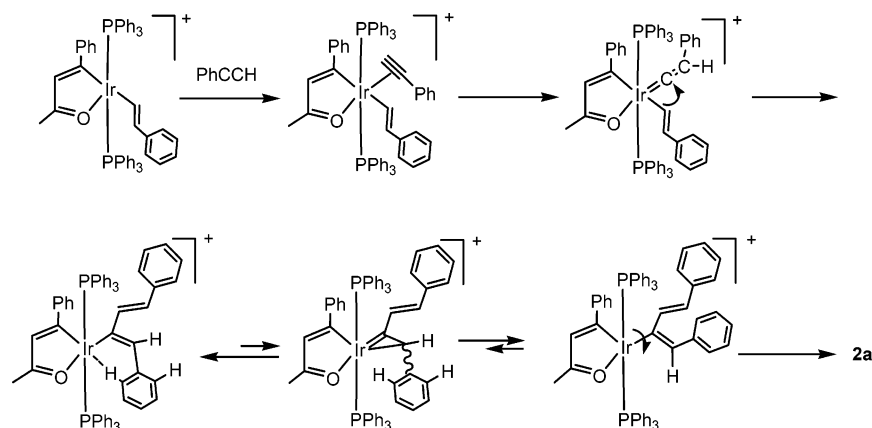
η^2 -Butadienyl **7** is a direct analogue of **2a** ($\text{X} = \text{H}$), and like **2a** ($\text{X} = \text{H}$), the $^{13}\text{C}\{^1\text{H}\}$ NMR spectrum of **7** shows a characteristic high-field signal for $\text{C}(\text{sp}^2)$ at δ 100.6 (s) that is assigned to C(13). The trans arrangement about the $\text{C}(12)=\text{C}(13)$ bond in the butadienyl group was clearly indicated by the mutual coupling of the two $\text{HC}(12)=\text{C}(13)\text{H}$ protons in ^1H NMR spectrum (CD_2Cl_2) at δ 6.42 ($^3J_{\text{HH}} = 16.0$ Hz, 1H) and 5.38 ($^3J_{\text{HH}} = 16.0$ Hz, 1H).

On the basis of its very similar NMR spectral characteristics, a similar C–H agostic intermediate was also found in the reaction between **1** and 2 equiv of $o\text{-CF}_3\text{-C}_6\text{H}_4\text{C}\equiv\text{CH}$ in CD_2Cl_2 (Scheme 4). The intermediate, formed in 88% yield after 15 min at 0°C , was characterized by ^1H , ^{31}P , and ^{19}F NMR spectroscopy, notably from its broad C–H aryl resonance at δ 3.67 (1H). Warming to room temperature led to a mixture of agostic **8** (minor) and η^2 -butadienyl **9** (major) in equilibrium, which was confirmed by the fact that the same ratio of **8** to **9** was obtained from isolated **9** or with

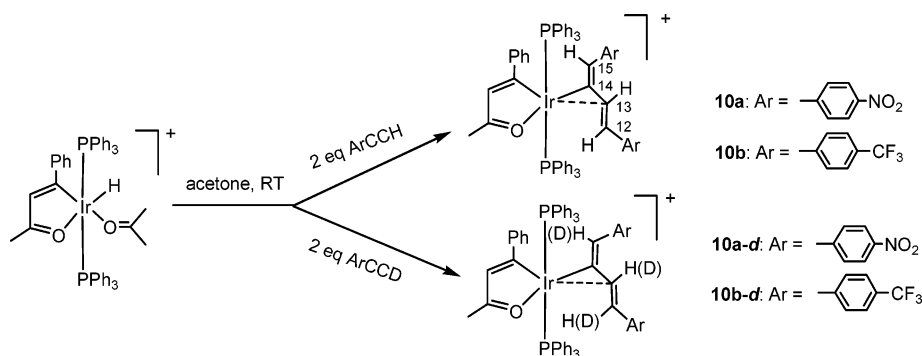
(18) (a) O'Connor, J. M.; Pu, L.; Rheingold, A. L. *J. Am. Chem. Soc.* **1987**, *109*, 7578. (b) O'Connor, J. M.; Hiibner, K.; Closson, A.; Gantzel, P. *Organometallics* **2001**, *20*, 1482.

(19) (a) Vignalok, A.; Milstein, D. *Acc. Chem. Res.* **2001**, *34*, 798. (b) van der Boom, M. E.; Iron, M. A.; Atasoylu, O.; Shimon, L. J. W.; Rozenberg, H.; Ben-David, Y.; Konstantinovski, L.; Martin, J. M. L.; Milstein, D. *Inorg. Chim. Acta* **2004**, *357*, 1854. (c) Albeniz, A. C.; Schulte, G.; Crabtree, R. H. *Organometallics* **1992**, *11*, 242.

Scheme 5



Scheme 6



temperature perturbation followed by relaxation. This suggests that these two weak interactions are of comparable strength. Because of its lower solubility, **9** could be isolated in solid form. Complex **9** could be characterized spectroscopically only from the mixture. In particular the ^1H NMR spectrum of **9** shows two trans CH vinyl protons ($^3J_{\text{HH}} = 15.8$ Hz) at δ 6.57 and 5.65. The $^{19}\text{F}\{^1\text{H}\}$ NMR spectrum of **9** shows two singlets with equal intensity at δ -59.55 and -59.58 . No acceptable $^{13}\text{C}\{^1\text{H}\}$ NMR spectrum of **9** could be obtained due to its poor solubility and its equilibration with **8**. The equilibrium constant (K_{eq}) was measured by ^{31}P NMR spectroscopy in CD_2Cl_2 : 22.7 at 21 $^\circ\text{C}$, 17.8 at 28 $^\circ\text{C}$, and 13.7 at 35 $^\circ\text{C}$. At higher temperatures the sample decomposed, and at lower temperatures the longer reaction time made the data less reliable.

The agostic complex **8** is therefore a kinetic intermediate leading to the more thermodynamically stable η^2 -butadienyl **9**. We propose that it is formed by the migratory insertion of the vinyl group to the least hindered side of the vinylidene ligand, anti to the β -Ph group (Scheme 5), possibly because there is free rotation around the iridium–vinylidene bond.¹⁰ This causes the Ph group to approach the iridium in a cis geometry for agostic interaction. Rearrangement of this agostic complex to the more stable final η^2 -butadienyl complex most likely goes through an η^2 -vinyl intermediate (Scheme 1 (a)).⁶

The kinetic isotope effect for the double insertion of $\text{PhCH}_2\text{C}\equiv\text{CH}$ was determined from a competition between $\text{PhCH}_2\text{C}\equiv\text{CH}$ and $\text{PhCH}_2\text{C}\equiv\text{CD}$ for reaction with **1** in CH_2Cl_2 . ^1H NMR data show a $k_{\text{H}}/k_{\text{D}}$ of 1.5 for the first alkyne to vinylidene rearrangement, but 1.0 for the second. This suggests that the C–H bond breaking

required in this rearrangement is not rate-determining. The results are consistent with the rate-determining slippage of an $\eta^2(\text{C}–\text{C})$ -alkyne intermediate to an $\eta^2(\text{C}–\text{H})$ -agostic species (path (b), Scheme 1), as suggested in previous theoretical studies.⁷

2.2. Double Insertion of Relatively Electron-Poor Alkynes. Surprisingly, moving to electron-withdrawing groups as alkyne substituents led to a change of mechanism. Two equivalents of such alkynes $\text{ArC}\equiv\text{CH}$ ($\text{Ar} = p\text{-C}_6\text{H}_4\text{CF}_3$, $p\text{-C}_6\text{H}_4\text{NO}_2$) were allowed to react with **1** in acetone (Scheme 6). As we expected, the reaction afforded η^2 -butadienyl **10a,b** from alkyne double insertion, although at a lower rate than for $\text{PhC}\equiv\text{CH}$ (Scheme 6). The nature of the η^2 -butadienyl products was readily confirmed by ^1H , ^{13}C , and ^{31}P NMR spectroscopy and elemental analyses. In particular, the $^{13}\text{C}\{^1\text{H}\}$ NMR spectra of **10a** and **10b** show characteristic peaks at δ 111.4 and 106.7, respectively, assigned to C(12). In addition, the $^{19}\text{F}\{^1\text{H}\}$ NMR spectrum of **10b** gives two singlets (δ -63.08 and -63.64) with equal intensity for the two CF_3 groups.

The mechanistic change was evident from isotope labeling experiments using $\text{ArC}\equiv\text{CD}$ ($\text{Ar} = p\text{-C}_6\text{H}_4\text{CF}_3$, $p\text{-C}_6\text{H}_4\text{NO}_2$), which indicated that deuterium fully scrambled into the three methine positions [C(12), C(13), and C(15)] of the butadienyl ligand. Similarly, addition of 2 equiv of $\text{PhC}\equiv\text{CH}$ to a CH_2Cl_2 solution of a related iridium hydride **11** also afforded the η^2 -butadienyl double insertion product **12** with the same scrambling pattern.

Complex **12** was fully characterized by ^1H , ^{31}P , and ^{13}C NMR spectroscopy, elemental analysis, and X-ray crystallography (Figure 3, Tables 1 and 2). The X-ray crystal structure of **12** shows that the geometry about

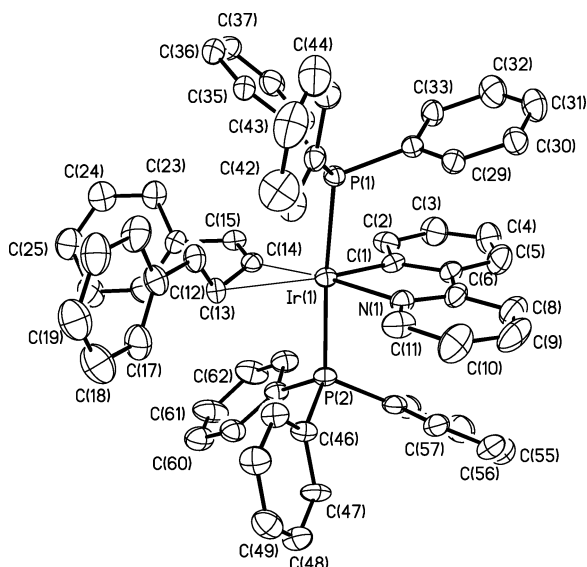


Figure 3. ORTEP diagram of the cation of **12** shown with 50% probability ellipsoids.

the iridium center is octahedral, with five normal tightly bound ligands and a sixth at a much longer distance, corresponding to a weak secondary interaction. This weak Ir...C(13) bond (2.504(6) Å) is ca. 0.5 Å longer than the normal Ir-C(14) bond (2.029(6) Å), while Ir...C(12) (3.11 Å) is outside the first coordination sphere. The C(12)-C(13) double bond (1.336(8) Å) is slightly elongated and is comparable to the C-C bonds in the aromatic rings (1.337-1.415 Å). The C(12)-C(13) double bond is highly twisted (86.7°) and deconjugated from the C(14)-C(15) bond. All these crystal data are closely comparable to those reported for **2a** (X = H).⁴

The scrambling of deuterium to the three possible positions in the butadienyl group suggests that the mechanism of the double insertion of these alkynes very likely involves a C-H oxidative addition step. The mechanism of the double insertion of *p*-CF₃(C₆H₄)C≡CD into **1** was investigated by ¹H NMR spectroscopy at

Table 2. Selected Bond Lengths and Angles for Complex 12

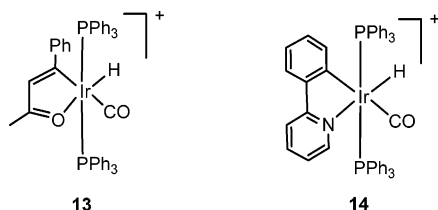
Bond Lengths (Å)	
Ir(1)-P(1)	2.361(2)
Ir(1)-P(2)	2.365(2)
Ir(1)-N(1)	2.175(5)
Ir(1)-C(1)	2.009(6)
Ir(1)-C(13)	2.504(6)
Ir(1)-C(14)	2.029(6)
C(12)-C(13)	1.336(8)
C(13)-C(14)	1.474(8)
C(14)-C(15)	1.326(8)
Bond Angles (deg)	
P(1)-Ir(1)-P(2)	175.53(5)
C(13)-Ir(1)-C(14)	36.1(2)
C(1)-Ir(1)-N(1)	78.3(2)
C(1)-Ir(1)-C(14)	109.0(2)
C(12)-C(13)-C(14)	122.7(5)
C(13)-C(14)-C(15)	126.8(5)

-5 °C. After 30 min, when the alkyne and the iridium hydride were still the only detectable species, deuterium scrambling between them was already observed. The deuteration of the free alkyne went from 98% to 88% in the reaction mixture, while that of the iridium hydride went from the natural abundance (~ 0%) to 24%. This scrambling was also confirmed by ²H NMR spectroscopy (46.0 MHz, CH₂Cl₂, -5 °C), where the Ir-D resonance at δ -20.8 was clearly observed. These results indicate a reversible oxidative addition of the alkyne to the iridium hydride.²⁰ This would afford an Ir^{III}(HD) or an Ir^V(H)(D) intermediate, which can undergo either C-H or C-D reductive elimination to lead to deuterium scrambling in the starting materials. A detailed mechanism of this double insertion is hard to study experimentally, since reversible C-H oxidative addition is the source of the deuterium scrambling and any later step will not change this feature. However, the direct insertion mechanism (path (a), Scheme 1) is unlikely since no reaction was observed between complex **1** and excess MeC≡CPh and PhC≡CPh, where the Me group in MeC≡CPh or the Ph group in PhC≡CPh would be expected to behave as spectators during a direct inser-

Table 1. Crystallographic Data for 12, 15a and 18a

	12 ·acetone	15a	18a ·Et ₂ O
empirical formula	C ₆₆ H ₅₇ F ₆ IrNOP ₂ Sb	C ₅₀ H ₄₄ F ₆ IrO ₃ P ₂ Sb	C ₆₀ H ₅₈ BF ₄ IrO ₃ P ₂
molecular weight (g mol ⁻¹)	1370.02	1182.74	1168.01
radiation, λ (Å)		Mo Kα (monochr), 0.71073 Å	
T (°C)	23	-100	-100
cryst syst	monoclinic	monoclinic	triclinic
space group	P2 ₁ /n (No. 14)	C2 (No. 5)	P1̄ (No. 2)
a (Å)	11.857(2)	25.032(5)	13.6505(3)
b (Å)	35.049(7)	14.670(3)	15.9723(4)
c (Å)	14.543(3)	13.062(3)	21.6001(6)
α (deg)	90	90	76.77(3)
β (deg)	97.79(3)	107.35(3)	78.30(3)
γ (deg)	90	90	83.67(3)
V (Å ³)	5988(2)	4578.5(16)	2481.1(9)
Z	4	4	2
D _{calcd} (g cm ⁻³)	1.520	1.716	1.563
μ(Mo Kα) (cm ⁻¹)	27.85	36.30	28.18
cryst size (mm)	0.30 × 0.20 × 0.20	0.15 × 0.15 × 0.10	0.20 × 0.20 × 0.20
total, unique no. of rflns	20 137, 12 946	9690, 9690	20 679, 12 176
R _{int}	0.032	0.000	0.0363
no. of observations used	12 946	9690	12 176
no. of params, restrictions	683, 4	597, 1	624, 7
R ^a , R _w ^b	0.0485; 0.116	0.0359; 0.0684	0.0365; 0.0788
GOF	1.041	1.043	1.036
min., max. resid dens (e Å ⁻³)	-1.07, 1.33	-1.782, 0.601	-1.44, 0.789

^a $R = \sum ||F_o| - |F_c|| / \sum |F_o|$, for all $I > 2\sigma(I)$. ^b $R_w = [\sum w(|F_o| - |F_c|)^2 / \sum w F_o^2]^{1/2}$.

**Figure 4.**

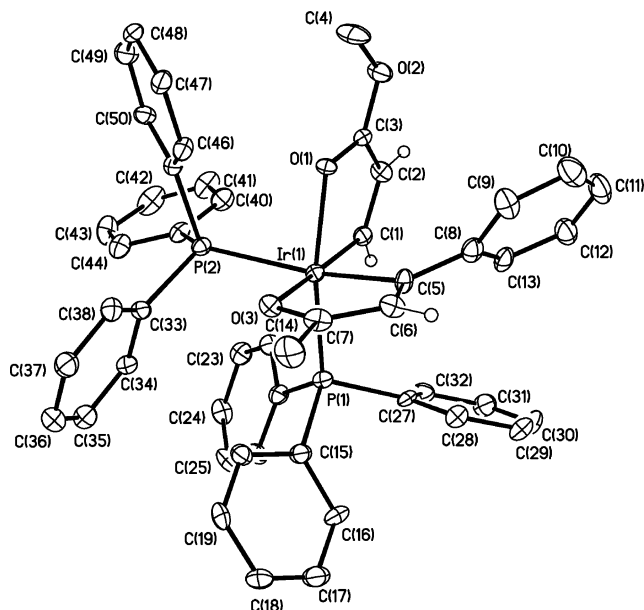
tion pathway. Therefore, both the intraligand 1,2-H shift pathway (path (b), Scheme 1) and the C-H oxidative addition followed by 1,3-H shift pathway (path (c), Scheme 1) are possible. Electrospray mass spectroscopy of the reaction mixture **10b-d** confirmed that all the four possible masses were present, corresponding to **10b-d₀** (4.6%), **10b-d₁** (24.7%), **10b-d₂** (43.4%), and **10b-d₃** (27.2%), based on analysis of the isotope patterns.

The contrast between the mechanisms of the insertion of PhC≡CH into **1** and into **11** may be due to electronic differences, because steric differences at the alkyne binding site are small. Investigation of the electronic differences was carried out by bubbling CO through CH₂Cl₂ solutions of **1** and **11** to yield carbonyls **13** and **14**, respectively (Figure 4). The CO stretching frequencies in IR spectroscopy, a sensitive indicator of the electronic character of **1** and **11**, show that **11** ($\nu_{\text{CO}} = 2042 \text{ cm}^{-1}$ for CO adduct **14**) is much more electron-rich than **1** ($\nu_{\text{CO}} = 2052 \text{ cm}^{-1}$ for **13**) and should therefore favor oxidative addition. The nature of the alkyne substituents also plays a role: oxidative addition should be favored by electronegative RC≡C groups, as is indeed the case for electron-poor aryl alkynes.

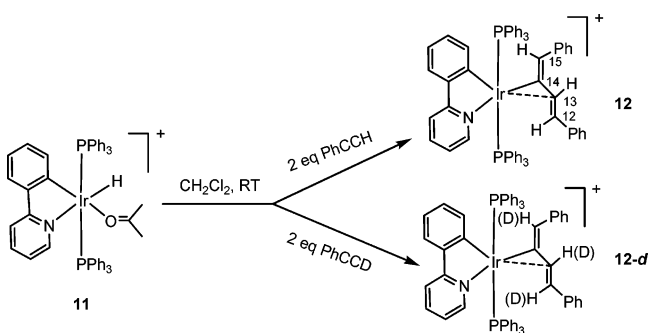
2.3. Insertion of Activated Alkynes into Hydride

1. Activated alkynes [HC≡CC(O)R] are also electron-poor, but they are much more polarized than the alkynes discussed above. The addition of 2 equiv of HC≡CC(O)OMe into a CH₂Cl₂ solution of **1** afforded an orange solution, from which the simple vinyl **15a** was isolated (89%) as a yellow solid upon addition of ether (Scheme 8). Here, the substrate carbonyl group plays the role of MeCN in the works described above, preventing subsequent reaction with another equivalent of alkyne. In the ¹H NMR spectra (CD₂Cl₂) of **15a**, a characteristic low-field resonance at δ 10.80 (dd, ³J_{HH} = 7.8 Hz, ³J_{PH} = 4.1 Hz), which became a doublet (³J_{HH} = 7.8 Hz) upon ³¹P decoupling, was assigned to C(1)–H on the basis of the carbenoid character of C(1) in the resultant iridafuran. C(2)–H resonates at δ 6.20 (dt, ³J_{HH} = 7.8 Hz, ⁴J_{PH} = 1.5 Hz). The ³¹P{¹H} NMR spectrum of this complex shows two mutually coupled doublets (10 Hz). This suggests that the two PPh₃ ligands are in a cis orientation, an extremely rare situation for the [IrH₂(PPh₃)₂]⁺ fragment. Furthermore, in the ¹³C{¹H} NMR spectrum (CD₂Cl₂), C(1) gives a triplet at δ 179.3 (²J_{PC} = 6.0 Hz) equally coupled to two cis phosphine ligands. In contrast, C(5) in the other iridafuran gives a doublet of doublets at δ 212.3 (²J_{PC} = 84 Hz, ²J_{PC} = 7.4 Hz) due to both trans (84 Hz) and cis (7.4 Hz) P–Ir–C coupling. Both ¹H and ¹³C NMR show that only one alkyne unit is incorporated into the product, even with 2 equiv of alkyne. An analogous product, **15b**, is also observed when **1** reacts with HC≡CC(O)Me. It is rather rare to

(20) For reversible alkyne C–H oxidative addition, see: Birk, R.; Berke, H.; Huttner, G.; Zsolnai, L. *Chem. Ber.* **1988**, *121*, 471.

**Figure 5.** ORTEP diagram of the cation of **15a** shown with 50% probability ellipsoids.

Scheme 7



have cis monodentate bisphosphine products derived from trans bisphosphine starting materials without any cis enforcer such as Cp or Cp*.^{9a,21}

X-ray single-crystal analysis further confirmed this proposed structure of **15a** and that the insertion is anti (Figure 5, Tables 1 and 3). Complex **15a** crystallized in the C-centered monoclinic space group C2 with one molecule in the asymmetric unit and four molecules in the unit cell. The geometry about the iridium atom can best be described as a slightly distorted octahedron. The bite-angles of the chelating ligands are 78.2(2)° and 77.8(2)° for O(1)–Ir(1)–C(1) and O(3)–Ir(1)–C(5), respectively, and a strong trans-effect for C(5) is observed, as the Ir(1)–P(2) bond is 0.15 Å longer than the Ir(1)–P(1) bond which is trans to O(1). The strong trans-effect of C(5) is due to its carbenoid character, consistent with highly low-field resonance of C(5) in ¹³C NMR spectroscopy. The two PPh₃ ligands are indeed cis to each other, and the large angle (100.51(6)°) is no doubt due to the steric repulsion. The backbone of both chelating ligands is essentially planar, and the phenyl ring, C(8)–13, is offset from this plane by 50.6°.

(21) (a) Chin, C. S.; Oh, M.; Won, G.; Cho, H.; Shin, D. *Polyhedron* **1999**, *18*, 811. (b) Thompston, J. S.; Bernard, K. A.; Rappol, J. P.; Atwood, J. D. *Organometallics* **1990**, *9*, 2727. (c) Drouin, M.; Harrod, J. F. *Inorg. Chem.* **1983**, *22*, 999. (d) Harrod, J. F.; Hamer, G.; Yorke, W. J. *Am. Chem. Soc.* **1979**, *101*, 3987. (e) Longato, B.; Morandini, F.; Bresadola, S. *Inorg. Chem.* **1976**, *15*, 650.

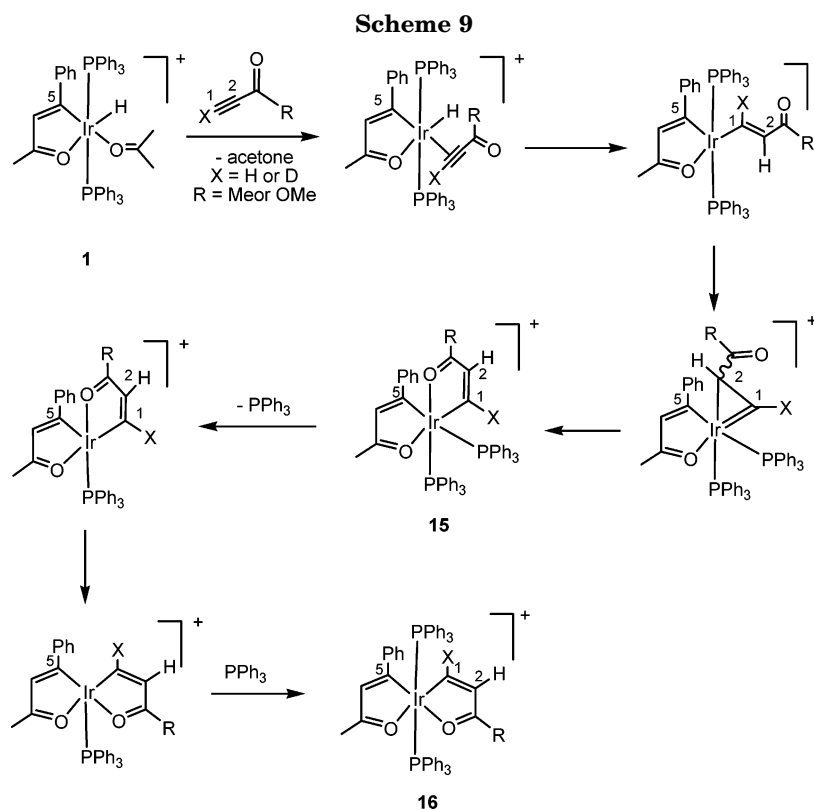
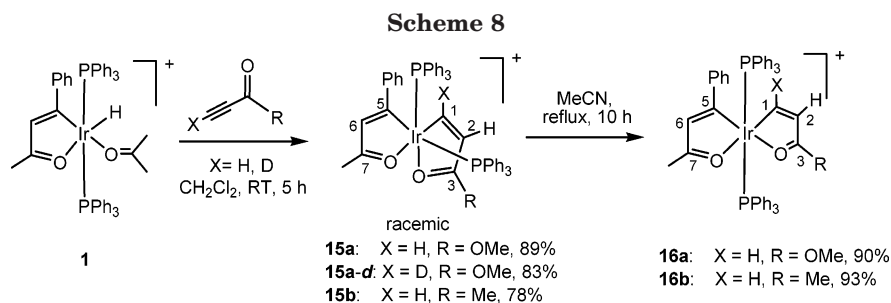


Table 3. Selected Bond Lengths and Angles for Complex 15a

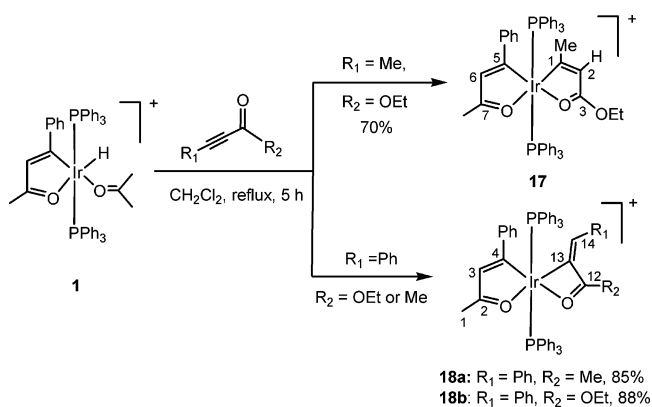
Bond Lengths (Å)	
Ir(1)–P(1)	2.275(1)
Ir(1)–P(2)	2.424(2)
Ir(1)–O(1)	2.147(3)
Ir(1)–O(3)	2.142(4)
Ir(1)–C(1)	2.004(6)
Ir(1)–C(5)	2.079(5)
C(5)–C(6)	1.349(8)
Bond Angles (deg)	
P(1)–Ir(1)–P(2)	100.51(6)
C(1)–Ir(1)–O(1)	78.2(2)
C(5)–Ir(1)–O(3)	77.8(2)

Prolonged reaction led to cis to trans isomerization; the trans product observed in ^1H and ^{31}P NMR spectroscopy is identical to **16a**, obtained by heating **15a** in acetonitrile under reflux. In the ^1H NMR spectrum of **16a**, a low-field resonance at δ 10.16 (d, $^3J_{\text{HH}} = 7.8$ Hz) is again assigned to the C(1)–H of the iridafuran. The $^{31}\text{P}\{^1\text{H}\}$ NMR spectrum of **16a** shows a singlet, consistent with a trans phosphine. The $^{13}\text{C}\{^1\text{H}\}$ NMR spectrum gives further support: C(5) gives a triplet at δ 200.9 ($^2J_{\text{PC}} = 7.0$ Hz) and C(1) another triplet at δ 181.7 ($^2J_{\text{PC}} = 7.2$ Hz). Virtual coupling for the ^{13}C NMR signal

of the *ipso*-carbon of the triphenylphosphine ligands is also consistent with trans-PPh₃ groups.

The deuterium labeling pattern is entirely different from before, indicating another mechanism functions in this case. When D–C≡CC(O)OMe reacts with **1**, the resultant vinyl **15a-d** gives ^1H NMR data indicating that deuterium remains bound to the same carbon C(1), and there is essentially no scrambling (<4%). This result is inconsistent with an alkyne to vinylidene rearrangement (path (b) or (c), Scheme 1), but supports a direct insertion mechanism (Scheme 9), resembling that proposed in a tungsten case.¹¹ Coordination of the alkyne, followed by an insertion into the Ir–H, affords a five-coordinate syn-insertion intermediate. An η^2 -vinyl intermediate then isomerizes this initial syn-insertion intermediate to the anti one. In this intermediate (**15**), carbene C(1), alkyl C(2), and carbene/vinyl C(5) are all high trans-effect ligands, and either C(1) or C(2) must be unfavorably located trans to C(5) if the PPh₃ ligands remain in their usual trans arrangement. Rearrangement to the cis phosphine system at this stage avoids these unfavorable interactions. This step is followed by the coordination of the carbonyl oxygen to yield the observed kinetic product **15a**. The fact that **15a** is the only product obtained even with 2 equiv of HC≡CC(O)–

Scheme 10



OMe suggests that the cis–trans isomerization of the vinyl group and subsequent oxygen binding must be faster than the insertion of a second equivalent of the alkyne because the double-insertion product that would be formed is not seen. Dissociation of the more labile PPh₃ in **15a** is expected to yield another fluxional five-coordinate intermediate. Rearrangement of the chelating ligands and recoordination of the PPh₃ affords the thermodynamic product **16a**.

Since the insertion of these alkynes into **1** involved no alkyne to vinylidene rearrangement, internal alkynes are also expected to undergo this reaction. Indeed, the reaction between **1** and Me–C≡CCO₂Et directly yielded **17** (Scheme 10), a trans phosphine complex, with no cis phosphine intermediate ever being observed. Similarities were found between the ¹³C{¹H} NMR spectra of **17** and **16a,b**.

A related internal alkyne, Ph–C≡CC(O)Me, reacts with **1**, however, to give a different vinyl product, **18a** (Scheme 10), by insertion in different regio- and stereochemistry. The choice of this alkyne simplifies the elucidation of the final product: the insertion of this alkyne would generate a symmetrical bis-iridafuran if the insertion pathway for **16a,b** or **17** is followed. In fact, only **18a** was obtained. In the ¹H NMR spectrum, the two methyl groups are distinct, and in the ¹³C{¹H} NMR spectrum, a triplet at δ 197.2 and another triplet at δ 112.0 were clearly assigned to the iridafuran carbon C(4) and the vinyl carbon C(13), respectively. The ¹³P{¹H} NMR spectrum (CD₂Cl₂) of **18a** shows a singlet at δ 6.48.

An X-ray crystal structure analysis confirmed the proposed structure for **18a** (Figure 6, Tables 1 and 4). The high trans-effect carbene/vinyl C(4) is cis to the vinyl C(13). The Ir(1)–C(4) bond is slightly (0.05 Å) shorter than the Ir(1)–C(13) bond, and the Ir(1)–O(2) bond is 0.1 Å longer than Ir(1)–O(1). The four-membered iridacycle is essentially planar, and the O(2)–Ir–C(13) bite-angle is very acute (62.08°). The P(1)–Ir(1)–P(2) angle is 170.35°. The formation of **18a** is clearly from a direct syn insertion with different regiochemistry. This insertion pattern was reported before only for terminal or symmetrical internal activated alkynes in Ir,¹² Ru,¹³ Os,^{13c,14,22} and W¹¹ hydrides.

To distinguish between electronic and steric effects, Ph–C≡CCO₂Et, electronically similar to Me–C≡CCO₂–

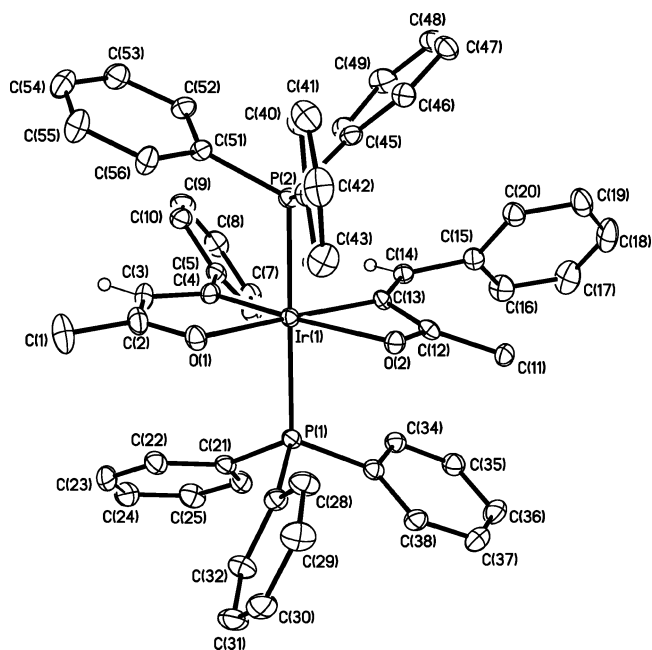


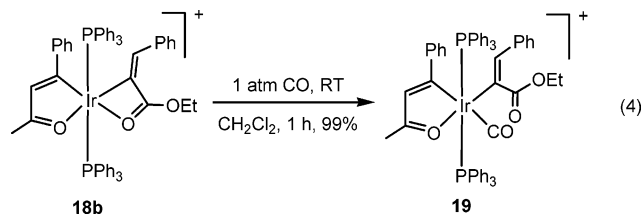
Figure 6. ORTEP diagram of the cation of **18a** shown with 50% probability ellipsoids.

Table 4. Selected Bond Lengths and Angles for Complex **18a**

Bond Lengths (Å)	
Ir(1)–P(1)	2.373(1)
Ir(1)–P(2)	2.373(1)
Ir(1)–C(4)	1.994(3)
Ir(1)–C(13)	2.048(3)
Ir(1)–O(1)	2.173(2)
Ir(1)–O(2)	2.272(2)
C(13)–C(14)	1.341(5)
Bond Angles (deg)	
P(1)–Ir(1)–P(2)	170.35(3)
C(4)–Ir(1)–O(1)	78.15(12)
C(13)–Ir(1)–O(2)	62.08(11)
Ir(1)–C(13)–C(12)	95.3(2)
Ir(1)–O(2)–C(12)	91.3(2)
C(13)–C(14)–C(15)	125.0(3)

Et, but sterically similar to Ph–C≡CC(O)Me, was allowed to react with **1**. As we expected, **18b**, an analogue of **18a**, was isolated, as clearly observed in ¹³C NMR spectroscopy, where a triplet at δ 197.6 is assigned to C(4) and another triplet at δ 103.8 is assigned to the vinyl carbon C(13). Comparison between insertion of Ph–C≡CC(O)OEt and Me–C≡CC(O)OEt into **1** (Scheme 10) highlights the role of steric effects, which reverse the direction of the insertion to put the bulky phenyl group one bond further away from the metal than would be the case by analogy with **17**; the phenyl group also ends up trans with respect to the metal for the same reason.

The ligand in the four-membered iridacycle would be expected to be hemilabile, because the carbonyl oxygen might readily dissociate. Indeed, bubbling CO (1 atm) slowly converts **18b** to **19** within 1 h (eq 4), but no



(22) Bohanna, C.; Callejas, B.; Edwards, A. J.; Esteruelas, M. A.; Lahoz, F. J.; Oro, L. A.; Ruiz, N.; Valero, C. *Organometallics* **1998**, *17*, 373.

reaction was found for **18a** under the same reaction conditions, indicating that the more basic ketone carbonyl oxygen is more tightly bonded than the ester one.

3. Conclusions

These results show that three different mechanisms for alkyne insertion are possible in this system, with the outcome being determined by a delicate balance of steric and electronic effects. The results also show that, in such cases, it can be dangerous to extend conclusions based on a single mechanistic study to apparently closely related cases. For relatively electron-rich alkynes, double insertion occurs with two independent alkyne to vinylidene rearrangements to afford η^2 -butadienyls. In the first insertion of these alkynes, deuterium labeling and crossover experiments confirmed that the alkyne to vinylidene rearrangement is intraligand. Both a vinyl intermediate and a vinylidene intermediate were trapped and isolated respectively during the first alkyne insertion. For the second alkyne insertion, a C–H agostic intermediate was isolated. For insertion of relatively electron-poor alkynes into **1**, double insertion was also observed. Deuterium labeling experiments show that we have a rare case of reversible alkyne C–H oxidative addition preceding insertion. Insertion of highly polarized alkynes $[R_1C\equiv CC(O)R_2]$ to **1** occurs only once and involves no vinylidene intermediates even when $R_1 = H$. The regio- and stereochemistry in this case are mainly controlled by the steric hindrance of the R_1 group. In this series, rare *cis*-(PPh_3)₂ intermediates were isolated in the insertion of highly polarized terminal alkynes $[HC\equiv CC(O)R]$, $R = Me$ or OMe into **1**. X-ray crystal structures of representative products were reported.

4. Experimental Section

General Considerations. All reactions were carried out under argon, although most of the products proved to be air stable. CH_2Cl_2 was distilled from CaH_2 under N_2 . Acetone was used without further purification. 2-Ethynylbenzyl alcohol²³ and iridium hydrides **1** and **5**⁴ were prepared as previously described. $PhC\equiv CD$ (98% D) and all other nondeuterated organic chemicals were purchased from Aldrich without further purification. ¹H and ¹³C NMR spectra were recorded on Bruker 400 or 500 spectrometers, and chemical shifts are reported with respect to $SiMe_4$. ³¹P NMR spectra were recorded on Bruker 400 spectrometers with external 85% H_3PO_4 standard. ²H NMR spectra were recorded on a GE Ω 300 spectrometer using CD_2Cl_2 as an external standard. Elemental analyses were performed at Atlantic Microlabs. X-ray diffraction for single crystals was measured on a Nonius KappaCCD diffractometer. IR spectra were recorded on a Midac M1200 spectrometer.

Preparation of Deuterated Alkynes. $MeOC(O)C\equiv CD$ was synthesized according to a literature report.²⁴ $PhCH_2C\equiv CD$, *p*- $MeO(C_6H_4)C\equiv CD$, *p*- $CF_3(C_6H_4)C\equiv CD$, and *p*- $NO_2(C_6H_4)C\equiv CD$ were synthesized from their corresponding protonated alkynes. To stirred CH_2Cl_2 (8 mL) solutions of these protonated alkynes (4.0 mmol) were added D_2O (20 mL) and $NaOD$ (40% solution in D_2O , 0.015 mL, 0.21 mmol). The resultant mixtures were left to stir for 3 days, followed by quenching with DCl

(37% solution in D_2O , 0.02 mL). The two layers were separated, and the aqueous layer was extracted with CH_2Cl_2 (8 mL). The CH_2Cl_2 layers were combined and dried over anhydrous Na_2SO_4 , followed by removal of CH_2Cl_2 under reduced pressure. ¹H NMR analysis indicated $\geq 98\%$ deuteration of the β -H in each alkyne.

General Procedure for the Synthesis of 2a–c (SbF_6^-). To a stirred solution of the **1** (SbF_6^- , 120 mg, 0.104 mmol) in CH_2Cl_2 (6 mL) was added 2 equiv of alkyne via syringe. The color of the solutions changed immediately from yellow to dark orange. The solutions were then stirred for 2 h at room temperature and were concentrated to ca. 0.5 mL under reduced pressure. Diethyl ether (15 mL) was then added to give yellow powders, which were washed with diethyl ether (2×20 mL), filtered, and dried *in vacuo*.

trans-Bis(triphenylphosphine)(η^2 -{O,C1}-1-phenylbut-1-en-3-on-1-yl)(1,4-diphenylbuta-1,4-dien-2-yl)iridium(III) hexafluoroantimonate [2a (SbF_6^- , X = H)]: yield 86%. ¹H NMR [500 MHz, 298 K, $CO(Me)_2-d_6$]: δ 7.62 (t, ³ $J_{H,H} = 7.4$ Hz, 1H), 7.38–7.58 (m, 33H), 7.18 (d, ³ $J_{HH} = 7.8$ Hz, 2H), 7.12 (t, ³ $J_{HH} = 7.7$ Hz, 2H), 7.04 (m, 3H), 6.82 (d, ³ $J_{HH} = 7.4$ Hz, 2H), 6.42 (d, ³ $J_{HH} = 16.2$ Hz, 1H, H(12)), 6.31 (d, ³ $J_{HH} = 7.3$ Hz, 2H), 5.92 (s, 1H, iridafuran C-H), 5.72 (d, ⁴ $J_{HH} = 1.6$ Hz, H(15)), 5.59 (dd, ³ $J_{HH} = 16.2$ Hz, ⁴ $J_{HH} = 1.6$ Hz, 1H, H(13)), 1.83 (t, $J_{P,H} = 1.5$ Hz, CH_3). ¹³C{¹H} NMR (100 MHz, CD_2Cl_2 , 298 K): δ 213.0 (s, C=O), 196.6 (t, $J_{P,C} = 5.7$ Hz, iridafuran Ir-C), 145.5 (s), 138.2 (s, iridafuran C-H), 137.8 (s), 135.6 (t, $J_{PC} = 5.2$ Hz), 134.9 (s), 133.7 (s, C(12)), 132.7 (t, $J_{PC} = 6.8$ Hz, C(14)), 131.5 (s), 130.6 (s), 129.6 (t, $J_{PC} = 5.1$ Hz), 129.3 (s), 129.1 (s), 128.7 (s), 128.6 (s), 128.3 (br s, C(15)), 127.4 (s), 127.0 (t, $J_{PC} = 28.0$ Hz, *ipso*- PPh_3), 126.7 (s), 100.3 (s, C(3)), 26.6 (s, CH_3). ³¹P{¹H} NMR (161.9 MHz, CD_2Cl_2 , 298 K): δ 4.79 (s). Anal. Calcd for $C_{62}H_{52}F_6IrOP_2Sb$: C, 57.15; H, 4.02. Found: C, 56.98; H, 4.00.

trans-Bis(triphenylphosphine)(η^2 -{O,C1}-1-phenylbut-1-en-3-on-1-yl)(1,4-dibenzylbuta-1,4-dien-2-yl)iridium(III) hexafluoroantimonate [2b (SbF_6^- , X = H)]: yield 92%. ¹H NMR [500 MHz, 298 K, $CO(Me)_2-d_6$]: δ 7.50–7.62 (m, 7 H), 7.40–7.48 (m, 24H), 7.38 (t, ³ $J_{HH} = 7.8$ Hz, 2H), 7.24–7.30 (m, 5H), 7.10–7.16 (m, 3H), 7.02 (d, ³ $J_{HH} = 7.9$ Hz, 2H), 6.63 (m, 2H), 6.14 (s, 1H, iridafuran C-H), 5.29 (dt, ³ $J_{HH} = 15.2$ Hz, ³ $J_{HH} = 7.2$ Hz, 1H, H(12)), 4.92 (br d, ³ $J_{HH} = 15.2$ Hz, 1H, H(13)), 4.82 (td, $J_{H,H} = 7.1$ Hz, $J_{H,H} = 1.6$ Hz, 1H, H(15)), 2.92 (d, $J_{H,H} = 7.1$ Hz, 2H, CH_2 vicinal to H(15)), 2.33 (d, ³ $J_{HH} = 6.9$ Hz, 2H, CH_2 vicinal to H(12)), 1.86 (s, 3H, CH_3). ¹³C{¹H} NMR (100 MHz, CD_2Cl_2 , 298 K): 213.3 (s, C=O), 201.7 (t, $J_{P,C} = 6.1$ Hz, iridafuran Ir-C), 145.5 (s), 141.3 (s), 138.0 (s), 137.8 (s), 135.5 (t, $J_{PC} = 5.1$ Hz, PPh_3), 132.4 (s), 131.6 (s), 129.7 (s), 129.6 (s, C(12)), 129.5 (s), 129.4 (t, $J_{PC} = 5.3$ Hz, PPh_3), 129.3 (s), 129.2 (s), 129.0 (s), 128.7 (s), 127.8 (t, $J_{P,C} = 27.5$ Hz, *ipso*- PPh_3), 127.4 (s), 126.7 (s), 126.4 (t, $J_{PC} = 6.3$ Hz, C(14)), 124.6 (br s, C(15)), 99.4 (br s, C(13)), 40.3 (s, CH_2), 39.7 (s, CH_2), 26.6 (s, CH_3). ³¹P{¹H} NMR [161.9 MHz, acetone-*d*₆, 298 K]: δ 2.21 (s). Anal. Calcd for $C_{64}H_{56}F_6IrOP_2Sb$: C, 57.75; H, 4.24. Found: C, 57.99; H, 4.56.

trans-Bis(triphenylphosphine)(η^2 -{O,C1}-1-phenylbut-1-en-3-on-1-yl)(1,4-di-*p*-methoxyphenylbuta-1,4-dien-2-yl)iridium(III) hexafluoroantimonate [2c (SbF_6^- , X = H)]: recrystallized from CH_2Cl_2 and diethyl ether, yield 85%. ¹H NMR [400 MHz, 298 K, $CO(Me)_2-d_6$]: δ 7.35–7.65 (m, 33H), 7.16 (d, ³ $J_{HH} = 7.4$ Hz, 2H), 6.76 (d, ³ $J_{HH} = 8.7$ Hz, 2H), 6.68 (d, ³ $J_{HH} = 8.7$ Hz, 2H), 6.61 (d, ³ $J_{HH} = 8.7$ Hz, 2H), 6.38 (d, ³ $J_{HH} = 16.0$ Hz, 1H, H(12)), 6.23 (d, ³ $J_{HH} = 8.7$ Hz, 2H), 5.94 (s, 1H, iridafuran CH), 5.66 (s, 1H, H(15)), 5.32 (d, ³ $J_{HH} = 16.0$ Hz, 1H, H(13)), 3.83 (s, 3H, OCH_3), 3.70 (s, 3H, OCH_3), 1.82 (s, 3H, CH_3). ¹³C{¹H} NMR [125.8 MHz, $(CD_3)_2C(O)$, 298 K]: δ 213.6 (s), 198.4 (t, $J_{PC} = 6.2$ Hz, iridafuran Ir-C), 162.6 (s), 159.4 (s), 146.4 (s), 138.8 (s), 137.0 (s), 136.2 (t, $J_{PC} = 5.1$ Hz, PPh_3), 132.9 (s, PPh_3), 131.8 (s), 131.5 (s), 131.2 (s), 131.1 (t, $J_{PC} = 6.5$ Hz, C(14)), 130.1 (t, $J_{PC} = 5.0$ Hz, PPh_3), 129.72 (s), 129.70 (s), 129.0 (s), 128.4 (s), 127.9 (t, $J_{PC} = 27.2$, *ipso*- PPh_3),

(23) Nugent, B. M.; Williams, A. L.; Prabhakaran, E. N.; Johnston, J. N. *Tetrahedron* **2003**, *59*, 8877.

(24) Labuschagne, A. J. H.; Schneider, D. F. *Tetrahedron Lett.* **1983**, *24*, 743.

115.5 (s), 114.6 (s), 96.5 (s, C(13)), 56.3 (s, OCH₃), 55.8 (s, OCH₃), 26.6 (s, CH₃). ³¹P{¹H} NMR [161.9 MHz, (CD₂)₂C(O), 298 K]: δ 5.70 (s). Anal. Calcd for C₆₄H₅₆F₆IrO₃P₂Sb·0.5CH₂-Cl₂·0.5O(CH₂CH₃)₂: C, 55.37; H, 4.33; Cl, 2.46. Found: C, 55.34; H, 4.37; Cl, 2.45. The stoichiometry of CH₂Cl₂ and Et₂O was further confirmed by ¹H NMR spectroscopy.

Syntheses of **2a–c** (SbF₆⁻, X = D) are essentially the same for those of **2a–c** (X = H) with comparable yields. The ¹H NMR (400 MHz, 298 K, acetone-*d*₆) of **2a** (X = D) is essentially the same as that of **2a** (X = H) except that δ 6.42 (H(12)) and 5.72 (H(15)) are missing (<4% for both) and 5.59 (H(13)) becomes a singlet. The ¹H NMR (400 MHz, 298 K, acetone-*d*₆) of **2b** (X = D) is essentially the same as that of **2b** (X = H) except that δ 5.29 (H(12)) and 4.82 (H(15)) are missing (<4% for both) and 4.92 (H(13)) becomes a singlet. The ¹H NMR (400 MHz, 298 K, acetone-*d*₆) of **2c** (X = D) is essentially the same as that of **2c** (X = H) except that δ 6.38 (H(12)) and 5.66 (H(15)) are missing (<3% for both) and δ 5.32 (H(13)) becomes a singlet.

Crossover Experiment Using PhCH₂C≡CH and PhC≡CD. To a stirred solution of **1** (SbF₆⁻, 200 mg, 0.173 mmol, in 5 mL of CH₂Cl₂) was added a mixture of PhCCD (21.4 mg, 0.207 mmol) and PhCH₂CCH (16.1 mg, 0.138 mmol) at room temperature. The solution changed from light yellow to dark orange immediately, and it was stirred for 48 h, after which the volatiles were removed in vacuo to yield a yellow solid. The solid was then washed with 3 × 15 mL of pentane within the reaction flask and dried in vacuo. Yield: 207 mg (91% based on **1**). The solid was then dissolved in ca. 1 mL of CD₂-Cl₂, and ca. 0.1 mL of this solution was used for NMR (¹H and ³¹P) analysis. A mixture of the four possible complexes (Figure 1) was characterized by ³¹P NMR. ³¹P{¹H} NMR (161.9 MHz, CD₂Cl₂, 298 K): δ 7.56 (s, **A**); 4.80 (s, **B**); 2.21 (s, **C**); and 0.11 (s, **D**). The ratio was **A**:**B**:**C**:**D** = 1.00:1.56:0.76:0.73 from their ³¹P NMR signal integrations. Complex **B** is **2a** (X = D) and complex **C** is **2b** (X = H), whose ¹H NMR spectra were known. By comparison with the ¹H NMR (400 MHz, CD₂Cl₂, 298 K) spectra of the products obtained from **1** and the mixture of PhCCH and PhCH₂CCH, partial assignment is possible. **A**: δ 6.18 (d, proton residue, 0.04H, H(12)), 5.73 (s, 1H, iridafuran C-H), 5.52 (s, 1H, H(13)), 4.78–4.85 (m, overlapping of H(15) of **A** and H(15) of **C**), 2.97 (d, ³J_{HH} = 6.8 Hz, 2H, CH₂C(15)); **B**: neither 6.42 (H(12)) nor 5.72 (H(15)) showed any proton residue (<3%); **D**: δ 5.67 (s, proton residue, 0.04H, H(15)), 5.24–5.34 (m, overlapping of H(12) of **D** and H(12) of **C**), 5.08 (d, ³J_{HH} = 15.2 Hz, 1H, H(13)), 2.40 (d, ³J_{HH} = 7.2 Hz, 2H, CH₂C(12)). ²H NMR (76.77 MHz, 298 K, acetone-*d*₆) of the mixture: broad and overlapping signals between δ 5.5 and 6.6, absence of any signal between δ 3.0 and 6.0 (no D-12 in **C** or **D** and no D-15 in **A** or **C**).

trans-Bis(triphenylphosphine)(η²-{O,C1}-1-phenylbut-1-en-3-on-1-yl)(acetonitrile)(2-phenylvinyl)iridium(III) hexafluoroantimonate [3 (SbF₆⁻)]. To a stirred solution of **1** (SbF₆⁻, 200 mg, 0.173 mmol) in CH₂Cl₂ (6 mL) was added acetonitrile (0.3 mL). The solution was stirred for 0.5 h before all the volatiles were removed under reduced pressure (ca. 0.1 mmHg) to give a yellow powder, which was then dissolved in CH₂Cl₂ (7 mL), followed by addition of phenylacetylene (18 mg, 0.176 mmol). The solution was stirred at 23 °C for 8 h, during which time the color of the solution changed from light yellow to orange. All the volatile was then removed in vacuo to give a tarry residue, to which was added diethyl ether (60 mL). The yellow ether solution was collected by filtration, and removal of diethyl ether afforded a yellow powder, which was recrystallized twice in diethyl ether to afford the analytically pure product. Yield: 98 mg (45%). ¹H NMR (400 MHz, 298 K, CD₂Cl₂, 298 K): δ 8.22 (dt, ³J_{HH} = 16.0 Hz, ³J_{PH} = 3.0 Hz, 1H, Ir-CH), 7.39–7.48 (m, 7H), 7.24–7.33 (m, 26H), 7.19 (t, ³J_{HH} = 8.0 Hz, 2H), 7.05 (t, ³J_{HH} = 7.3 Hz, 1H), 6.97 (d, ³J_{HH} = 7.6 Hz, 2H), 6.85 (d, ³J_{HH} = 7.2 Hz, 2H), 6.44 (s, 1H, iridafuran CH), 5.85 (d, ³J_{HH} = 16.0 Hz, 1H, IrCH=CHPh), 1.55 (s, 3H, Me), 1.45 (s, 3H, Me). ¹³C{¹H} NMR (100.6 MHz, 298 K, CD₂-

Cl₂, 298 K): δ 212.6 (s, C=O), 204.5 (t, ³J_{PC} = 7.4 Hz, iridafuran Ir-C), 147.3 (s), 140.9 (s), 140.6 (s), 135.7 (t, ³J_{PC} = 5.0 Hz, PPh₃), 131.8 (s, PPh₃), 130.2 (s), 129.02 (s), 129.00 (s), 128.8 (t, ³J_{PC} = 5.2 Hz, PPh₃), 126.7 (t, ³J_{PC} = 27.1 Hz, *ipso*-PPh₃), 126.0 (s), 125.3 (s), 121.8 (s, MeCN), 118.4 (t, ³J_{PC} = 8.9 Hz, IrCH), 25.5 (s, CH₃), 3.17 (s, CH₃CN). ³¹P{¹H} NMR (161.9 MHz, CD₂Cl₂, 298 K): δ 0.06 (s). Anal. Calcd for C₅₆H₄₉F₆-IrNOP₂Sb: C, 54.16; H, 3.98; N, 1.13. Found: C, 54.49; H, 3.88; N, 1.10.

trans-Bis(triphenylphosphine)(η²-{O,C1}-1-phenylbut-1-en-3-on-1-yl)(4,5-benzo-2-oxacyclohexylidene)(hydrido)iridium(III) hexafluoroantimonate [4 (BF₄⁻)]. To a stirred solution of **1** (BF₄⁻, 87 mg, 0.086 mmol) in CH₂Cl₂ (2 mL) was added a CH₂Cl₂ solution (4 mL) of 2-ethynylbenzyl alcohol (23 mg, 0.174 mmol). The solution was stirred for 4 h at 23 °C, followed by concentration to ca. 0.5 mL under reduced pressure. Diethyl ether was then added, and the mixture was scratched to give a light yellow powder, which was recrystallized using CH₂Cl₂ and diethyl ether. Yield: 75 mg (80%). ¹H NMR (400 MHz, CD₂Cl₂, 295 K): δ 6.90–7.30 (m, 35 H), 6.83 (t, 8.0 Hz, 2H), 6.79 (d, 6.4 Hz, 1H), 6.56 (d, 5.6 Hz, 1H), 6.52 (s, 1H), 4.54 (s, 2H, CH₂), 3.50 (s, 2H, CH₂), 1.83 (s, 3H, CH₃), -20.94 (t, 13.6 Hz, 1H, Ir-H). ¹³C{¹H} NMR (100 MHz, CD₂-Cl₂, 298 K): δ 292.5 (t, 7.0 Hz, Ir=C), 228.3 (t, 10 Hz, Ir-C), 213.5 (s), 146.3 (s), 137.6 (s), 134.4 (t, 5.4 Hz), 131.7 (s), 130.9 (s), 130.3 (s), 129.7 (t, 28 Hz), 129.0 (t, 5.1 Hz), 128.5 (s), 128.0 (s), 127.9 (s), 126.7 (s), 126.3 (s), 124.8 (s), 79.4 (s, CH₂), 59.6 (s, CH₂), 26.8 (s). ³¹P{¹H} NMR (161.9 MHz, CD₂Cl₂, 295 K): δ 15.32 (s). Anal. Calcd for C₅₅H₄₈BF₄IrO₂P₂: C, 61.06; H, 4.47. Found: C, 60.78; H, 4.46.

Complex 6 (SbF₆⁻). To the stirred solution of **1** (SbF₆⁻, 249 mg, 0.215 mmol) in 5 mL of CH₂Cl₂ was added phenylacetylene (44 mg, 0.431 mmol) at room temperature. The solution changed from light yellow to dark red immediately. The resulting solution was stirred for 15 min before it was quickly concentrated to ca. 0.5 mL in vacuo. Diethyl ether (20 mL) was added to the solution, and a yellow precipitate formed. This precipitate was filtered, washed with Et₂O (3 × 10 mL), and dried in vacuo. Yield: 254 mg (0.195 mmol, 91%). Slow diffusion of ether to the dichloromethane solution of **6** (SbF₆⁻) after 1 day at room temperature afforded an orange plate crystal of **6** suitable for X-ray diffraction, together with a yellow powder of **7** (SbF₆⁻). ¹H NMR (400 MHz, 298 K, CD₂Cl₂): δ 7.61 (d, ³J_{HH} = 8.0 Hz, 1H), 7.02–7.45 (m, 38 H), 6.82 (t, ³J_{HH} = 8.0 Hz, 1H), 6.80 (t, ³J_{HH} = 8.0 Hz, 1H), 6.58 (AB d, ³J_{HH} = 16.0 Hz, 1H), 6.57 (d, ³J_{HH} = 8.2 Hz, 1H), 6.50 (AB d, ³J_{HH} = 16.0 Hz, 1H), 5.20 (br s, 2H, agostic C-H), 2.38 (t, ³J_{HH} = 6.4 Hz, 2H, CH₂), 2.23 (t, ³J_{HH} = 6.2 Hz, 2H, CH₂), 1.31 (m, 2H, CH₂). ¹H NMR (400 MHz, 198 K, CD₂Cl₂): 7.47 (t, ³J_{HH} = 6.8 Hz, 1H), 7.44 (d, ³J_{HH} = 8.0 Hz, 1H), 6.90–7.40 (m, 37H), 6.78 (t, ³J_{HH} = 8.2 Hz, 1H), 6.71 (t, ³J_{HH} = 8.4 Hz, 1H), 6.55 (d, ³J_{HH} = 16.0 Hz, 1H), 6.54 (br s, 1H, deoalesced pendant agostic C-H), 6.46 (d, ³J_{HH} = 7.2 Hz, 1H), 6.37 (d, ³J_{HH} = 16.0 Hz, 1H), 3.80 (br s, 1H, actual agostic C-H), 2.38 (br s, 2H, CH₂), 2.12 (br s, 2H, CH₂), 1.22 (br s, 2H, CH₂). ¹³C{¹H} NMR (100 MHz, CD₂Cl₂, 193 K): δ 214.7 (s, C=O), 149.0 (s), 148.8 (s), 144.3 (t, ³J_{PC} = 7.0 Hz, Ir-C), 143.2 (t, ³J_{PC} = 6.7 Hz, Ir-C), 140.0 (s), 139.7 (br s), 137.4 (br s), 136.8 (br s), 136.4 (s), 136.3 (s), 133.9 (br s, P(C₆H₅)₃), 131.7 (s), 130.7 [br s, P(C₆H₅)₃], 130.3 (s), 128.7 (s), 127.8 [br s, P(C₆H₅)₃], 127.0 (s), 126.6 (br s, deoalesce pendant agostic C-H), 126.1 [t, ³J_{HP} = 27.0 Hz, *ipso*-PPh₃], 126.1 (s, overlapping, confirmed by DEPT45) 125.6 (s), 125.1 (s), 122.6 (s), 107.2 (br s, agostic C-H), 36.5 (s, CH₂), 27.3 (s, CH₂), 22.3 (s, CH₂). ³¹P{¹H} NMR (161.9 MHz, CD₂Cl₂, 298 K): δ 3.09 (s). Anal. Calcd for C₆₂H₅₂F₆IrOP₂Sb: C, 57.15; H, 4.02. Found: C, 56.78; H, 4.04.

Complex 7 (SbF₆⁻). Complex **6** (SbF₆⁻, 100 mg, 0.0767 mmol) was dissolved in CH₂Cl₂ (5 mL), and the solution was heated under reflux for 12 h, after which it was concentrated to ca. 0.5 mL, followed by addition of Et₂O (20 mL). A yellow precipitate formed and was filtered. It was then washed with

Et₂O (2 × 15 mL) and dried in vacuo. Yield: 89 mg (0.068 mmol, 89%). ¹H NMR (400 MHz, 298 K, CD₂Cl₂): δ 8.10 (d, ³J_{HH} = 7.6 Hz, 1H), 7.34–7.40 (m, 7H), 7.31 (t, ³J_{HH} = 7.6 Hz, 1H), 7.13–7.25 (m, 26H), 7.10 (t, ³J_{HH} = 7.2 Hz, 1H), 7.04 (t, ³J_{HH} = 7.6 Hz, 2H), 6.91 (d, ³J_{HH} = 8.0 Hz, 2H), 6.63 (d, ³J_{HH} = 7.2 Hz, 1H), 6.42 (d, ³J_{HH} = 16.0 Hz, 1H, H(12)), 6.34 (d, ³J_{HH} = 7.9 Hz, 2H), 6.22 (s, 1H, H(15)), 5.38 (d, ³J_{HH} = 16.0 Hz, 1H, H(13)), 2.16 (t, ³J_{HH} = 6.4 Hz, 2H, CH₂), 2.09 (t, ³J_{HH} = 6.0 Hz, 2H, CH₂), 1.11 (m, 2H, CH₂CH₂CH₂). ¹³C{¹H} NMR (100 MHz, CD₂Cl₂, 298 K): δ 215.7 (s, C=O), 152.0 (t, J_{PC} = 7.8 Hz, Ir-C), 150.8 (s), 143.7 (s), 138.1 (s), 137.0 (s), 135.1 (t, J_{PC} = 5.2 Hz, PPh₃), 134.9 (s), 133.5 (t, J_{P, C} = 6.6 Hz, C(14)), 133.0 (s), 131.9 (s), 129.9 (s), 129.5 (s), 129.3 (t, J_{PC} = 5.0 Hz, PPh₃), 128.9 (s), 128.5 (s), 127.7 (s), 127.4 (t, J_{PC} = 27.0 Hz, *ipso*-PPh₃), 127.3 (s), 126.7 (s), 126.0 (s, C(15)), 123.7 (s), 119.3 (s, C(12)), 100.6 (s, C(13)), 37.2 (s, CH₂), 28.4 (s, CH₂), 22.8 (s, CH₂). ³¹P{¹H} NMR (161.9 MHz, CD₂Cl₂, 298 K): δ 0.96(s). Anal. Calcd for C₆₂H₅₂F₆IrOP₂Sb: C, 57.15; H, 4.02. Found: C, 57.15; H, 4.27.

Observation of Complex 8 (SbF₆⁻). In an NMR tube, **1** (SbF₆⁻, 30 mg, 0.0259 mmol) was dissolved in CD₂Cl₂ (0.7 mL). To this solution was added via syringe *o*-CF₃C₆H₄C≡CH (5.6 mg, 0.052 mmol) at 20 °C. The ¹H, ³¹P, and ¹⁹F NMR spectra (CD₂Cl₂, 10 °C) were quickly (within 25 min) measured, and ³¹P and ¹⁹F NMR spectra indicated that the solution contained **8** (88%) and **9** (12%). Partial ¹H NMR (400 MHz, CD₂Cl₂, 283 K): δ 7.87 (s, 1H), 7.56 (d, ³J_{HH} = 8.0 Hz, 1H), 7.25 (t, ³J_{HH} = 7.6 Hz, 1H), 7.16 (t, ³J_{HH} = 7.4 Hz, 1H), 7.00 (d, ³J_{HH} = 16.0 Hz, 1H), 6.87 (m, 3.0 H), 6.58 (m, 2H), 6.07 (d, ³J_{HH} = 7.6 Hz, 1H), 5.57 (d, ³J_{HH} = 16.0 Hz), 5.24 (s, 1H), 3.67 (br s, 1H), 1.78 (s, 3H, CH₃). ³¹P{¹H} NMR (161.9 MHz, CD₂Cl₂, 283 K): δ 2.53. ¹⁹F{¹H} NMR (376.3 MHz, CD₂Cl₂, 283 K): δ -59.32 (s), -60.77 (s). Isolation of **8** (SbF₆⁻) was attempted, but only a mixture of **8** (SbF₆⁻) and **9** (SbF₆⁻) in a ratio of 3:1 was obtained.

trans-Bis(triphenylphosphine)(η²-{O,C1}-1-phenylbut-1-en-3-on-1-yl)(1,4-di-*o*-trifluoromethylphenylbuta-1,4-dien-2-yl)iridium(III) hexafluoroantimonate [9** (SbF₆⁻)].** To a stirred solution of **1** (SbF₆⁻, 150 mg, 0.130 mmol) in CH₂Cl₂ (6 mL) was added *o*-CF₃C₆H₄C≡CH (45 mg, 0.264 mmol) via syringe. The color of the solution changed from yellow to orange immediately. The solution was then stirred for 18 h at 28 °C before all the solvent was removed under reduced pressure to give a yellow tar, which was washed with ether (2 × 20 mL) until the ether solution was almost colorless. The ether solution was discarded, and a yellow powder was obtained, which was dissolved in CH₂Cl₂ (1 mL), quickly precipitated with ether (20 mL), filtered, and dried in vacuo. Yield: 120 mg (0.083 mmol, 64%). The ¹H NMR spectrum of this powder [**9** (SbF₆⁻)] was quickly measured. ¹H NMR (400 MHz, 298 K, CD₂Cl₂): δ 7.61 (t, ³J_{HH} = 7.5 Hz, 1H), 7.56 (d, ³J_{HH} = 7.8 Hz, 1H), 7.28–7.52 (m, 36H), 7.10 (t, ³J_{HH} = 7.6 Hz), 7.04 (m, 1H), 6.94 (t, ³J_{HH} = 7.6 Hz, 1H), 6.65 (d, ³J_{HH} = 15.6 Hz, 1H, H(12)), 6.43 (d, ³J_{HH} = 7.8 Hz, 1H), 6.10 (s, 1H), 5.91 (d, ³J_{HH} = 15.6 Hz, 1H, H(13)), 5.53 (s, 1H), 1.60 (s, 3H, CH₃). ³¹P{¹H} NMR (161.9 MHz, CD₂Cl₂, 298 K): δ 8.74. ¹⁹F{¹H} NMR (376.3 MHz, CD₂Cl₂, 298 K): δ -59.55 (s, 3F), 59.58 (s, 3F). Anal. Calcd for C₆₄H₅₀F₁₂IrOP₂Sb: C, 53.42; H, 3.50. Found: C, 53.29; H, 3.70.

Measurement of the K_{eq} between 8 (SbF₆⁻) and 9 (SbF₆⁻). In an NMR tube charged with a mixture of **8** (SbF₆⁻) and **9** (SbF₆⁻) in a ratio of 3:1 (18 mg) was added CD₂Cl₂ (0.7 mL). Enough time (6 h for 35 °C, 24 h for 28 °C, and 40 h for 21 °C) was allowed for the equilibrium to be reached. The [η²-butadienyl **9**]/[agostic **8**] ratio at equilibrium was measured to be 22.7, 17.8, and 13.7 at 21, 27, and 35 °C, respectively, based on ³¹P{¹H} NMR analysis.

trans-Bis(triphenylphosphine)(η²-{O,C1}-1-phenylbut-1-en-3-on-1-yl)(1,4-di-*p*-nitrophenylbuta-1,4-dien-2-yl)iridium(III) hexafluoroantimonate [10a** (SbF₆⁻)] and *trans*-Bis(triphenylphosphine)(η²-{O,C1}-1-phenylbut-1-en-3-**

on-1-yl)(1,4-di-*p*-trifluoromethylphenylbuta-1,4-dien-2-yl)iridium(III) hexafluoroantimonate [10b** (SbF₆⁻)].** To a stirred solution of the **1** (SbF₆⁻, 150 mg, 0.141 mmol) in acetone (6 mL) was added *p*-NO₂C₆H₄C≡CH (41.5 mg, 0.282 mmol). The solutions were stirred for 12 h at 23 °C, followed by concentration of the solution to ca. 0.5 mL. Diethyl ether (20 mL) was then added to the solution to give a yellow precipitate, which was then filtered and recrystallized using CH₂Cl₂ and diethyl ether. Yield for **10a** (SbF₆⁻): 143 mg (0.110 mmol, 78%). ¹H NMR (400 MHz, acetone-*d*₆, 283 K): δ 8.00 (d, ³J_{HH} = 8.5 Hz, 2H), 7.88 (d, ³J_{HH} = 8.4 Hz, 2H), 7.69 (t, ³J_{HH} = 7.5 Hz, 1H), 7.48–7.69 (m, 32H), 7.25 (d, ³J_{HH} = 7.4 Hz, 2H), 7.09 (d, ³J_{HH} = 8.5 Hz, 2H), 6.40 (d, ³J_{HH} = 16.4 Hz, 1H), 6.11 (d, ³J_{HH} = 16.4 Hz, 1H), 5.88 (s, 1H), 5.73 (s, 1H), 1.81 (s, 3H, CH₃). ¹³C{¹H} NMR (100 MHz, acetone-*d*₆, 298 K): δ 214.1 (s, CO), 190.2 (t, J_{PC} = 6.0 Hz, iridafuran Ir-C), 148.2 (s), 146.2 (s), 143.7 (s), 141.4 (t, J_{PC} = 6.9 Hz, C(14)), 141.3 (s), 138.4 (s), 135.7 (t, J_{PC} = 5.2 Hz, PPh₃), 133.0 (s, PPh₃), 131.8 (s), 130.6 (s), 130.0 (t, J_{PC} = 5.2 Hz, PPh₃), 129.6 (s), 129.4 (s), 128.8 (s), 128.2 (s), 128.1 (t, J_{PC} = 2.6 Hz, C(15)), 126.5 (t, J_{PC} = 28 Hz, *ipso*-PPh₃), 124.5 (s), 124.2 (s), 111.5 (s), 26.0 (s, CH₃). ³¹P{¹H} NMR (161.9 MHz, (CD₃)₂CO, 298 K): δ 8.01 (s, PPh₃), -142.1 (septet, ²J_{PF} = 708 Hz, PF₆⁻). Anal. Calcd for C₆₂H₅₀F₆IrN₂O₅P₃: C, 57.19; H, 3.87; N, 2.15. Found: C, 57.46; H, 4.24; N, 2.06. Complex **10a-d** (SbF₆⁻) was obtained at a comparable yield through a direct method analogous to the synthesis of **10a** (SbF₆⁻). The ¹H NMR spectrum of **10a-d** (SbF₆⁻) is similar to that of **10a** (SbF₆⁻) except for three peaks: δ 6.40 (m, 0.41H), 6.11 (m, 0.30H), and 5.73 (m, 0.30H).

The synthesis of **10b** (SbF₆⁻) is analogous to that of **10a** (SbF₆⁻), using **1** (SbF₆⁻, 150 mg, 0.130) and **2** equiv of *p*-CF₃C₆H₄C≡CH (45 mg, 0.265 mmol) in acetone or CH₂Cl₂ (6 mL). Yield: 142 mg (0.099 mmol, 76%). ¹H NMR (500 MHz, 298 K, CD₂Cl₂): δ 7.60 (t, ³J_{HH} = 7.5 Hz, 1H), 7.49 (t, ³J_{HH} = 7.3 Hz, 6H, *para*-PPh₃), 7.29–7.45 (m, 28H), 7.27 (d, ³J_{HH} = 8.1 Hz, 2H), 7.08 (d, ³J_{HH} = 8.1 Hz, 2H), 6.32 (d, ³J_{HH} = 15.6 Hz, 1H, H(14)), 6.30 (d, ³J_{HH} = 7.2 Hz, 2H), 5.70 (s, 1H), 5.64 (s, 1H), 5.59 (d, ³J_{HH} = 15.6 Hz, 1H, H(13)), 1.69 (s, 3H, CH₃). ¹³C{¹H} NMR (100 MHz, CD₂Cl₂, 298 K): δ 213.2 (s, CO), 192.3 (t, J_{PC} = 6.2 Hz, iridafuran Ir-C), 144.9 (s), 140.7 (s), 138.2 (s), 137.8 (s), 136.2 (t, J_{PC} = 6.7 Hz, C(14)), 135.2 (t, J_{PC} = 5.2 Hz, PPh₃), 132.5 (s, PPh₃), 131.5 (s), 130.6 (s), 129.4 (t, J_{PC} = 5.1 Hz, PPh₃), 129.2 (s), 128.5 (s), 127.8 (s), 127.6 (br s), 127.2 (s), 126.2 (t, J_{PC} = 27.7 Hz, *ipso*-PPh₃), 126.1 (q, J_{FC} = 3.7 Hz, C-CF₃), 125.5 (q, J_{FC} = 3.6 Hz, C-CF₃), 124.8 (q, J_{FC} = 27.1 Hz, CF₃), 124.5 (q, J_{FC} = 27.2 Hz, CF₃), 106.9 (br s, C(14)), 26.1 (s, CH₃). ³¹P{¹H} NMR (161.9 MHz, CD₂Cl₂, 298 K): δ 5.25 (s). ¹⁹F{¹H} NMR (376.3 MHz, CD₂Cl₂, 283 K): δ -63.02 (s, 3F, CF₃), -63.64 (s, 3F, CF₃). Anal. Calcd for C₆₄H₅₀F₁₂IrOP₂Sb: C, 53.42; H, 3.50. Found: C, 53.07; H, 3.57.

Complex **10b-d** (SbF₆⁻) was obtained at a comparable yield through a direct method analogous to the synthesis of **10b** (SbF₆⁻). The ¹H NMR spectrum of **10b-d** (SbF₆⁻) is similar to that of **10b** (SbF₆⁻) except for three peaks: δ 6.32 (m, 0.44H), 5.64 (s, 0.26H), and 5.59 (m, 0.29H). Electron-spray MS [molecular ion peaks, cation mode, mass (intensity)]: 1201.2 (3.46), 1202.2 (20.7), 1203.2 (51.6), 1204.2 (81.8), 1205.2 (100, normalized), 1206.2 (86.3), 1207.2 (40.4), 1208.2 (11.8), 1209.2 (3.0). Calculated mole percentage of **10b-d₀**, **10b-d₁**, **10b-d₂**, and **10b-d₃** is 4.6, 24.7, 43.4, and 27.2, respectively.

trans-Bis(triphenylphosphine)(2-*o*-pyridylphenyl)(acetone)(hydrido)iridium(III) hexafluoroantimonate [11** (SbF₆⁻)].** To a stirred solution of [Ir(H)₂(PPh₃)₂(acetone)₂]SbF₆ (300 mg, 0.280 mmol) in acetone (3 mL) was added via syringe 2-phenylpyridine (44 mg, 0.284 mmol). Bubbling and precipitation were immediately observed. Diethyl ether (15 mL) was then added to the suspension. The white precipitate was then filtered and washed with diethyl ether (15 mL). Yield: 294 mg (0.252 mmol, 90%). ¹H NMR (500 MHz, acetone-*d*₆, 298 K): δ 9.49 (s, 1H), 7.60 (t, ³J_{HH} = 7.5 Hz, 1H), 7.43 (m, 6H, PPh₃), 7.27–7.38 (m, 13H) 7.15–7.25 (m, 15H), 6.88 (t, ³J_{HH}

= 7.5 Hz, 1H), 6.49 (t, $^3J_{\text{HH}} = 7.1$ Hz, 1H), 2.11 (s, 6H, CH_3), -15.77 (t, $^2J_{\text{PH}} = 15.4$ Hz, Ir-H). $^{13}\text{C}\{^1\text{H}\}$ NMR (100 MHz, CD_2Cl_2 , 298 K): δ 164.2 (s), 148.1 (s), 144.5 (s), 141.6 (s), 137.5 (s), 134.1 (t, $J_{\text{PC}} = 5.5$ Hz, PPh_3), 132.7 (t, $J_{\text{PC}} = 8.6$ Hz, Ir-C), 131.0 (s, PPh_3), 129.9 (s), 128.8 (t, $J_{\text{PC}} = 5.2$ Hz, PPh_3), 128.3 (t, $J_{\text{PC}} = 26.5$ Hz, *ipso*- PPh_3), 125.3 (s), 122.9 (s), 122.2 (s), 119.9 (s), 31.7 (s, CH_3). $^{31}\text{P}\{^1\text{H}\}$ NMR (161.9 MHz, CD_2Cl_2 , 298 K): δ 17.35 (s). Anal. Calcd for $\text{C}_{50}\text{H}_{45}\text{F}_6\text{IrNOP}_2\text{Sb}$: C, 51.51; H, 3.89; N, 1.20; F, 9.78. Found: C, 51.52; H, 3.86; N, 1.26; F, 9.64.

trans-Bis(triphenylphosphine)(2-*o*-pyridylphenyl)(1,4-diphenylbuta-1,4-dien-2-yl)iridium(III) Hexafluoroantimonate [12 (SbF₆⁻) and 12-*d* (SbF₆⁻)]. To a stirred suspension of **11** (SbF₆⁻, 200 mg, 0.172 mmol) in CH_2Cl_2 (4 mL) was added $\text{PhC}\equiv\text{CH}$ (35 mg, 0.344 mmol). A red solution was quickly formed. The solution was stirred at 23 °C for 2 h before it was concentrated to ca. 0.5 mL. Diethyl ether (20 mL) was added to the solution, and an orange precipitate appeared, which was filtered, washed with ether (20 mL), and dried in vacuo. Yield: 180 mg (0.137 mmol, 80%). A crystal of **12** (SbF₆⁻) suitable for X-ray crystal structure analysis was obtained by careful layering of the acetone solution of **12** (SbF₆⁻) with pentane. ^1H NMR (500 MHz, CD_2Cl_2 , 298 K): δ 8.82 (d, $^3J_{\text{HH}} = 5.1$ Hz, 1H), 8.15 (d, $^3J_{\text{HH}} = 7.4$ Hz, 1H), 7.59 (t, $^3J_{\text{HH}} = 7.3$ Hz, 1H), 7.48 (t, $^3J_{\text{HH}} = 7.5$ Hz, 1H), 7.42 (t, $^3J_{\text{HH}} = 7.6$ Hz, 2H, Ph), 6.93–7.40 (m, 38 H), 6.80 (t, $^3J_{\text{HH}} = 7.4$ Hz, 1H), 6.58 (d, $^3J_{\text{HH}} = 7.4$ Hz, 2H, Ph), 6.52 (d, $^3J_{\text{HH}} = 7.4$ Hz, 1H), 6.37 (d, $^3J_{\text{HH}} = 15.8$ Hz, 1H, H(12)), 6.15 (s, 1H, H(15)), 5.74 (d, $^3J_{\text{HH}} = 15.8$ Hz, 1H, H(13)). $^{13}\text{C}\{^1\text{H}\}$ NMR (125.7 MHz, CD_2Cl_2 , 302 K): δ 164.1 (s), 153.3 (s), 143.9 (s), 143.0 (br s), 139.1 (s), 138.8 (s), 135.7 (s), 134.8 (t, $J_{\text{PC}} = 5.1$ Hz, PPh_3), 133.7 (s), 131.5 (s, PPh_3), 131.2 (s), 131.0 (s), 130.3 (s), 129.9 (s), 129.0 (t, $J_{\text{PC}} = 5.0$ Hz, PPh_3), 128.8 (t, $J_{\text{PC}} = 6.0$ Hz, C(14)), 128.2 (s), 128.1 (s, C(12)), 127.8 (t, $J_{\text{PC}} = 27.8$ Hz, *ipso*- PPh_3), 127.4 (s), 127.2 (br s, C(15)), 126.1 (s), 125.9 (s), 124.4 (s), 123.7 (s), 121.6 (s), 103.8 (s, C(13)). $^{31}\text{P}\{^1\text{H}\}$ NMR (161.9 MHz, CD_2Cl_2 , 298 K): δ 2.27 (s). Anal. Calcd for $\text{C}_{63}\text{H}_{51}\text{F}_6\text{IrNP}_2\text{Sb}\cdot\text{C}_3\text{H}_6\text{O}$: C, 57.86; H, 4.19; N, 1.02; Found: C, 58.29; H, 4.12; N, 1.16.

The synthesis of **12-*d*** (SbF₆⁻) followed the same method as that of **12** (SbF₆⁻), using **11** (SbF₆⁻, 200 mg, 0.172 mmol) and $\text{PhC}\equiv\text{CD}$ (36 mg, 0.349 mmol) in CH_2Cl_2 (4 mL). Yield: 168 mg (0.128 mmol, 75%). The ^1H NMR (500 MHz, CD_2Cl_2 , 298 K) data of **12-*d*** (SbF₆⁻) are the same as those of **12** (SbF₆⁻), except for three signals: δ 6.37 (m, 54% H, H(12)), 6.15 (s, 10% H, H(15)), 5.74 (m, 43% H, H(13)). ^2H NMR (76.8 MHz, CH_2Cl_2 , 298 K): δ 5.0–6.8 (m, br).

trans-Bis(triphenylphosphine)(η^2 -{O,C1}-1-phenylbut-1-en-3-on-1-yl)(carbonyl)(hydrido)iridium(III) Hexafluoroantimonate [13 (SbF₆⁻)]. To a solution of **1** (SbF₆⁻, 80 mg, 0.069 mmol) in CH_2Cl_2 (8 mL) was bubbled CO (1 atm) for 15 min. The solution was then concentrated to ca. 0.5 mL under reduced pressure, followed by precipitation using diethyl ether (15 mL). The light yellow powder was filtered and dried in vacuo. Yield: 75 mg (0.067 mmol, 96%). ^1H NMR (500.1 MHz, CD_2Cl_2 , 298 K): δ 7.55 (t, $^3J_{\text{HH}} = 7.1$ Hz, 6H, PPh_3), 7.37–7.47 (m, 24H), 7.25–7.29 (m, 3H), 7.08 (t, $^3J_{\text{HH}} = 7.7$ Hz, 2H), 6.79 (s, 1H, iridafuran CH), 1.90 (s, 3H, CH_3), -18.90 (t, $^2J_{\text{PH}} = 11.7$ Hz, Ir-H). $^{13}\text{C}\{^1\text{H}\}$ NMR (125.7 MHz, CD_2Cl_2 , 298 K): δ 219.7 (t, $J_{\text{PC}} = 9.2$ Hz, iridafuran Ir-C), 215.3 (s, iridafuran CO), 173.1 (t, $J_{\text{PC}} = 6.3$ Hz, CO), 142.2 (s), 136.2 (s), 134.4 (t, $J_{\text{PC}} = 5.7$ Hz, PPh_3), 132.5 (s, PPh_3), 132.2 (s), 131.5 (br s), 129.2 (t, $J_{\text{PC}} = 5.5$ Hz, PPh_3), 128.7 (s), 127.6 (t, $J_{\text{PC}} = 29.8$ Hz, PPh_3), 26.3 (s, CH_3). $^{31}\text{P}\{^1\text{H}\}$ NMR (161.9 MHz, CD_2Cl_2 , 298 K): δ 8.38 (s). IR (CH_2Cl_2 film): 2052 cm^{-1} (ν_{CO}). Anal. Calcd for $\text{C}_{47}\text{H}_{40}\text{F}_6\text{IrO}_2\text{P}_2\text{Sb}$: C, 50.10; H, 3.58. Found: C, 50.50; H, 3.74.

trans-Bis(triphenylphosphine)(2-*o*-pyridylphenyl)(carbonyl)(hydrido)iridium(III) Hexafluoroantimonate [14 (SbF₆⁻)]. To a solution of **11** (SbF₆⁻, 80 mg, 0.069 mmol) in CH_2Cl_2 (8 mL) was bubbled CO (1 atm) for 20 min. The

solution was then concentrated to ca. 0.5 mL under reduced pressure, followed by precipitation using diethyl ether (15 mL). The white powder was filtered and dried in vacuo. Yield: 77 mg (0.068 mmol, 98%). ^1H NMR (500.1 MHz, CD_2Cl_2 , 298 K): δ 8.81 (d, $^3J_{\text{HH}} = 5.5$ Hz, 1H), 7.53 (td, $^3J_{\text{HH}} = 8.0$ Hz, $^4J_{\text{HH}} = 1.5$ Hz, 1H), 7.40 (t, $^3J_{\text{HH}} = 7.5$ Hz, 6H, PPh_3), 7.25–7.35 (m, 12H), 7.05–7.22 (m, 16H), 6.99 (td, $^3J_{\text{HH}} = 7.8$ Hz, $^4J_{\text{HH}} = 1.0$ Hz, 1H), 6.62 (t, $^3J_{\text{HH}} = 7.5$ Hz, 1H), -15.26 (t, $^2J_{\text{PH}} = 12.5$ Hz, 1H, Ir-H). $^{13}\text{C}\{^1\text{H}\}$ NMR (125.7 MHz, CD_2Cl_2 , 298 K): δ 175.0 (t, $J_{\text{PC}} = 7.4$ Hz, CO), 165.0 (s), 153.3 (t, $J_{\text{PC}} = 10.7$ Hz, Ir-C), 147.4 (s), 143.3 (s), 138.7 (s), 133.9 (t, $J_{\text{PC}} = 5.4$ Hz, PPh_3), 131.9 (s, PPh_3), 131.2 (s), 129.1 (t, $J_{\text{PC}} = 5.2$ Hz, PPh_3), 128.2 (t, $J_{\text{PC}} = 29.1$ Hz, *ipso*- PPh_3), 126.7 (s), 124.9 (s), 124.6 (s), 121.1 (s). $^{31}\text{P}\{^1\text{H}\}$ NMR (161.9 MHz, CD_2Cl_2 , 298 K): δ 5.83 (s). IR (CH_2Cl_2 film): 2042 cm^{-1} (ν_{CO}). Comparisons of these data to those in previous literature confirmed the structure of **14** (SbF₆⁻).

cis-Bis(triphenylphosphine)(η^2 -{O,C1}-1-phenylbut-1-en-3-on-1-yl)(η^2 -{O,C1}-methylprop-1-enoat-1-yl)iridium(III) Hexafluoroantimonate [15a (SbF₆⁻) and 15a-*d* (SbF₆⁻)]. To a stirred solution of **1** (SbF₆⁻, 150 mg, 0.130 mmol) in CH_2Cl_2 (6 mL) was added $\text{HC}\equiv\text{CCO}_2\text{Me}$ (22 mg, 0.262 mmol) via syringe. The solution was then stirred at 23 °C for 8 h, during which time the color changed from light yellow to orange. The solution was then concentrated to ca. 0.5 mL, followed by slow addition of diethyl ether (15 mL). Yellow microcrystals formed, which were filtered and washed with diethyl ether (2 × 15 mL). Analytically pure **15a** (SbF₆⁻) was obtained by drying the microcrystal in vacuo. Yield: 136 mg (116 mmol, 89%). ^1H NMR (400 MHz, CD_2Cl_2 , 298 K): δ 10.80 (dd, $^3J_{\text{HH}} = 7.8$ Hz, $^3J_{\text{PH}} = 4.1$ Hz, 1H, IrCH), turned into a doublet ($^3J_{\text{HH}} = 7.8$ Hz in $^1\text{H}\{^{31}\text{P}\}$ NMR spectroscopy), 7.03–7.53 (m, 31H), 7.00 (t, $^3J_{\text{HH}} = 7.4$ Hz, 2H, Ph), 6.84 (d, $^4J_{\text{PH}} = 9.3$ Hz, 1H, iridafuran CH), turned into a singlet in $^1\text{H}\{^{31}\text{P}\}$ NMR spectroscopy), 6.32 (d, $^3J_{\text{HH}} = 7.4$ Hz, 2H, Ph), 6.20 (dt, $^3J_{\text{HH}} = 7.8$ Hz, $^4J_{\text{PH}} = 1.5$ Hz, 1H, IrCH=CH), 3.20 (s, 3H, OCH₃), 2.39 (s, 3H, CH₃). $^{13}\text{C}\{^1\text{H}\}$ NMR (125.7 MHz, CD_2Cl_2 , 298 K): δ 216.8 (d, $J_{\text{PC}} = 9.2$ Hz, ketone iridafuran C=O), 212.3 (dd, $J_{\text{PC}} = 84$ Hz, $J_{\text{PC}} = 7.5$ Hz, iridafuran Ir-CPh), 185.3 (d, $J_{\text{PC}} = 1.5$ Hz, ester CO), 179.3 (t, $J_{\text{PC}} = 6.0$ Hz, IrCH), 142.6 (s), 137.0 (s), 135.2 (d, $J_{\text{PC}} = 8.0$ Hz, PPh_3), 135.1 (d, $J_{\text{PC}} = 10.6$ Hz, PPh_3), 132.3 (d, $J_{\text{PC}} = 2.5$ Hz, PPh_3), 131.7 (d, $J_{\text{PC}} = 2.3$ Hz, PPh_3), 130.4 (s), 130.2 (d, $J_{\text{PC}} = 2.2$ Hz), 129.7 (d, $J_{\text{PC}} = 44$ Hz, *ipso*- PPh_3), 129.2 (d, $J_{\text{PC}} = 2.0$ Hz, PPh_3), 129.1 (d, $J_{\text{PC}} = 3.3$ Hz, PPh_3), 128.3 (dd, $J_{\text{PC}} = 62.7$ Hz, $J_{\text{PC}} = 2.2$ Hz, *ipso*- PPh_3), 127.9 (s), 124.0 (s), 55.1 (s, OCH₃), 26.9 (s, CH₃). $^{31}\text{P}\{^1\text{H}\}$ NMR (161.9 MHz, CD_2Cl_2 , 298 K): δ 0.20 (d, $J_{\text{PP}} = 10$ Hz, PPh_3), -11.40 (d, $J_{\text{PP}} = 10$ Hz, PPh_3). Anal. Calcd for $\text{C}_{50}\text{H}_{44}\text{F}_6\text{IrO}_2\text{P}_2\text{Sb}$: C, 50.77; H, 3.75. Found: C, 50.99; H, 3.79.

The synthesis of **15a-*d*** (SbF₆⁻) followed the same method as that of **15a** (SbF₆⁻), using **1** (SbF₆⁻ salt, 150 mg, 0.130 mmol) and $\text{DC}\equiv\text{CCO}_2\text{Me}$ (22 mg, 0.260 mmol) in CH_2Cl_2 (4 mL). Yield: 128 mg (0.108 mmol, 83%). The ^1H NMR (400 MHz, CD_2Cl_2 , 298 K) data of **15a-*d*** are the same as those of **15a**, except for two signals: δ 10.80 missing (IrCD, <5% H), 6.20 (s, IrCD=CH). ^2H NMR (76.77 MHz, CH_2Cl_2 , 298 K): δ 10.8 (s).

cis-Bis(triphenylphosphine)(η^2 -{O,C1}-1-phenylbut-1-en-3-on-1-yl)(η^2 -{O,C2}-pent-2-en-3-on-2-yl)iridium(III) Hexafluoroantimonate [15b (SbF₆⁻)]. The synthesis of **15b** (SbF₆⁻) is directly analogous to that of **15a** (SbF₆⁻) using **1** (SbF₆⁻, 120 mg, 0.104 mmol) and $\text{HC}\equiv\text{CC(O)Me}$ (14 mg, 0.026 mmol) in CH_2Cl_2 at 23 °C. Yield: 95 mg (0.081 mmol, 78%). ^1H NMR (400 MHz, CD_2Cl_2 , 298 K): δ 11.29 (dd, $^3J_{\text{HH}} = 7.2$ Hz, $^3J_{\text{PH}} = 3.6$ Hz, 1H, IrCH=CH), 7.00–7.50 (m, 31H), 6.97 (t, $^3J_{\text{HH}} = 7.6$ Hz, 2H, Ph), 6.74 (d, $^4J_{\text{PH}} = 9.2$ Hz, 1H, iridafuran CH), 6.62 (d, $^3J_{\text{HH}} = 7.2$ Hz, 1H, IrCH=CH), 6.35 (d, $^3J_{\text{HH}} = 7.6$ Hz, 2H, Ph), 2.35 (s, 3H, CH₃), 1.58 (d, $J_{\text{PH}} = 2.0$ Hz, 3H, CH₃). $^{13}\text{C}\{^1\text{H}\}$ NMR (100.6 MHz, CD_2Cl_2 , 298 K): 215.7 (d, $J_{\text{PC}} = 7.4$ Hz, CO), 212.4 (t, $J_{\text{PC}} = 2$ Hz), 211.8 (dd, $J_{\text{PC}} = 79.2$ Hz, $J_{\text{PC}} = 7.6$ Hz, IrCPh=), 198.5 (t, $J_{\text{PC}} = 5.6$ Hz,

IrCH), 143.9 (s), 137.8 (s), 136.4 (s), 134.7 (d, $J_{PC} = 2.6$ Hz, PPh₃), 134.6 (d, $J_{PC} = 2.6$ Hz, PPh₃), 131.8 (d, $J_{PC} = 2.5$ Hz, PPh₃), 131.2 (d, $J_{PC} = 2.0$ Hz, PPh₃), 129.9 (s), 129.1 (d, $J_{PC} = 2.2$ Hz), 128.7 (d, $J_{PC} = 6.7$ Hz, PPh₃), 128.60 (d, $J_{PC} = 6.1$ Hz, PPh₃), 128.57 (d, $J_{PC} = 45.4$ Hz, *ipso*-PPh₃), 127.9 (dd, $J_{PC} = 60.6$ Hz, $J_{PC} = 2.0$ Hz, *ipso*-PPh₃), 127.7 (s), 26.4 (s, CH₃), 23.7 (d, $J_{PC} = 4.1$ Hz, CH₃). ³¹P{¹H} NMR (161.9 MHz, CD₂Cl₂, 298 K): δ 4.73 (d, $J_{PP} = 11.6$ Hz, PPh₃), -11.40 (d, $J_{PP} = 11.7$ Hz, PPh₃). Anal. Calcd for C₅₀H₄₄F₆IrO₃P₂Sb: C, 51.47; H, 3.80. Found: C, 51.49; H, 3.80.

trans-Bis(triphenylphosphine)(η^2 -{O,C1}-1-phenylbut-1-en-3-on-1-yl)(η^2 -{O,C1}-methylprop-1-enoat-1-yl)iridium(III) Hexafluoroantimonate [16a (SbF₆⁻)]. Complex **15a** (SbF₆⁻, 100 mg, 0.084 mmol) was dissolved in acetonitrile (5 mL) and was refluxed for 10 h. The solvent was then removed under reduced pressure to give a yellow residue, which was washed with diethyl ether (15 mL) to give a yellow powder. Analytically pure **15a** (SbF₆⁻) was obtained by drying this powder in vacuo. Yield: 90 mg (0.076 mmol, 90%). ¹H NMR (400 MHz, CD₂Cl₂, 298 K): δ 10.17 (d, $^3J_{HH} = 7.8$ Hz, 1H, IrCH=CH), 7.10–7.65 (m, 33H), 7.05 (d, $^3J_{HH} = 7.2$ Hz, 2H, Ph), 6.39 (s, 1H, iridafuran CH), 6.00 (dt, $^3J_{HH} = 7.8$ Hz, $^3J_{PH} = 1.4$ Hz, 1H, IrCH=CH), 2.89 (s, 3H, OCH₃), 1.45 (t, $^5J_{PH} = 1.5$ Hz, CH₃). ¹³C{¹H} NMR (100.6 MHz, CD₂Cl₂, 298 K): δ 213.3 (s, ketone CO), 200.9 (t, $J_{PC} = 5.8$ Hz, IrCPh), 184.4 (s, ester CO), 181.7 (t, $J_{PC} = 7.2$ Hz, IrCH=CH), 147.2 (s), 138.8 (s), 135.5 (t, $J_{PC} = 5.2$ Hz, PPh₃), 132.2 (s, PPh₃), 130.8 (s), 129.6 (s), 129.0 (t, $J_{PC} = 5.2$ Hz, PPh₃), 127.9 (s), 126.0 (t, $J_{PC} = 27.8$ Hz, *ipso*-PPh₃), 123.8 (s), 54.3 (s, OCH₃), 25.1 (s, CH₃). ³¹P{¹H} NMR (161.9 MHz, CD₂Cl₂, 298 K): δ 9.44 (s). Anal. Calcd for C₅₀H₄₄F₆IrO₃P₂Sb: C, 50.77; H, 3.75. Found: C, 50.67; H, 3.62.

trans-Bis(triphenylphosphine)(η^2 -{O,C1}-1-phenylbut-1-en-2-on-1-yl)(η^2 -{O,C2}-pent-2-en-3-on-2-yl)iridium(III) Hexafluoroantimonate [16b (SbF₆⁻)]. The synthesis of **16b** (SbF₆⁻) is directly analogous to that of **16a** (SbF₆⁻) using 80 mg (0.069 mmol). Yield: 74 mg (0.063 mmol, 93%). ¹H NMR (400 MHz, CD₂Cl₂, 298 K): δ 10.81 (d, $^3J_{HH} = 7.5$ Hz, 1H, IrCH=CH), 7.42–7.52 (m, 7H), 7.30–7.38 (m, 14H), 7.18–7.26 (m, 12H), 7.09 (d, $^3J_{HH} = 7.5$ Hz, 2H, Ph), 6.59 (s, 1H, iridafuran CH), 6.47 (d, $^3J_{HH} = 7.5$ Hz, $^3J_{PH} = 1.2$ Hz, 1H, IrCH=CH), 1.42 (t, $^5J_{PH} = 2.0$ Hz, CH₃), 1.29 (t, $^5J_{PH} = 2.0$ Hz, CH₃). ¹³C{¹H} NMR (125.8 MHz, CD₂Cl₂, 298 K): δ 213.6 (s, CO), 213.4 (s, CO), 203.4 (t, $J_{PC} = 5.8$ Hz, IrCPh), 198.1 (t, $J_{PC} = 6.0$ Hz, IrCH), 147.6 (s), 139.0 (s), 137.9 (s), 135.6 (t, $J_{PC} = 5.1$ Hz, PPh₃), 132.2 (s, PPh₃), 130.7 (s), 129.5 (s), 128.9 (t, $J_{PC} = 5.2$ Hz, PPh₃), 128.0 (s), 125.8 (t, $J_{PC} = 30.2$ Hz, *ipso*-PPh₃), 25.0 (s, Me), 24.6 (s, Me). ³¹P{¹H} NMR (161.9 MHz, CD₂Cl₂, 298 K): δ 10.44 (s). Anal. Calcd for C₅₀H₄₄F₆IrO₂P₂Sb: C, 51.47; H, 3.80. Found: C, 51.39; H, 3.72.

trans-Bis(triphenylphosphine)(η^2 -{O,C1}-1-phenylbut-1-en-3-on-1-yl)(η^2 -{O,C2}-ethylbut-2-enoat-2-yl)iridium(III) Hexafluoroantimonate [17 (SbF₆⁻)]. To a stirred solution of **1** (SbF₆⁻, 85 mg, 0.073 mmol) in CH₂Cl₂ (5 mL) was added Me-C≡CCO₂Et (21 mg, 0.19 mmol). The solution was refluxed for 5 h, followed by concentration to ca. 0.5 mL. A yellow precipitate appeared upon addition of diethyl ether (10 mL). Analytically pure **17** was obtained by recrystallization using CH₂Cl₂ and diethyl ether. Yield: 62 mg (0.051 mmol, 70%). ¹H NMR (500 MHz, CD₂Cl₂, 295 K): δ 7.53 (t, $^3J_{HH} = 6.8$ Hz, 6H), 7.30–7.45 (m, 26H), 7.15 (t, $^3J_{HH} = 7.9$ Hz, 2H), 6.71 (d, $^3J_{HH} = 7.2$ Hz, 2H), 6.36 (s, 1H), 5.76 (s, 1H), 3.34 (q, $^3J_{HH} = 7.3$ Hz, 2H), 1.75 (s, 3H), 1.50 (t, $J_{PH} = 1.6$ Hz, 3H), 0.81 (t, $^3J_{HH} = 7.0$ Hz, 3H). ¹³C NMR (125 MHz, CD₂Cl₂, 295 K): δ 212.2 (s), 203.6 (t, $J_{PC} = 6.5$ Hz, iridafuran Ir-C), 191.2 (t, $J_{PC} = 7.7$ Hz, iridafuran Ir-C), 183.1 (s), 149.2 (s), 141.2 (s), 135.3 (t, $J_{PC} = 4.8$ Hz, PPh₃), 132.0 (s), 129.5 (s), 128.8 (t, $J_{PC} = 4.4$ Hz, PPh₃), 128.5 (s), 127.4 (s), 125.7 (t, $J_{PC} = 26.8$ Hz, *ipso*-PPh₃), 125.2 (s), 63.5 (s), 33.7 (s), 24.6 (s), 15.7 (s), 14.1 (s), 10.8 (s). ³¹P{¹H} NMR (161.9 MHz, CD₂Cl₂, 298 K): δ 4.93

(s). Anal. Calcd for C₅₂H₄₈F₆IrO₃P₂Sb: C, 51.58; H, 4.00. Found: C, 51.51; H, 3.94.

trans-Bis(triphenylphosphine)(η^2 -{O,C1}-1-phenylbut-1-en-3-on-1-yl)(η^2 -{O,C2}-1-phenylbut-1-(E)-en-3-one-2-yl)iridium(III) Tetrafluoroborate [18a (BF₄⁻)] and trans-Bis(triphenylphosphine)(η^2 -{O,C1}-1-phenylbut-1-en-3-on-1-yl)(η^2 -{O,C2}-ethylbut-2-(E)-enoat-2-yl)iridium(III) Hexafluoroantimonate [18b (SbF₆⁻)]. The synthesis of **18a** (BF₄⁻) is directly analogous to that of **17** using **1** (BF₄⁻, 101 mg, 0.100 mmol) and Ph-C≡C(O)Me (29 mg, 0.201 mmol). Yield: 85% (93 mg, 0.085 mmol). ¹H NMR (500 MHz, acetone-*d*₆, 295 K): δ 7.45–7.60 (m, 31H), 7.4 (t, $^3J_{HH} = 7.0$ Hz, 2H), 7.21–7.32 (m, 5H), 7.12 (s, 1H), 6.68 (d, $^3J_{HH} = 6.7$ Hz, 2H), 6.37 (s, 1H), 1.68 (s, 3H), 0.95 (s, 3H). ¹³C NMR (125 MHz, CD₂Cl₂, 295 K): δ 227.7 (s), 212.8 (s), 197.2 (t, $J_{PC} = 5.4$ Hz, iridafuran Ir-C), 148.8 (s), 147.8 (s), 139.0 (s), 138.4 (s), 135.5 (t, $J_{PC} = 5.4$ Hz, PPh₃), 132.2 (s), 131.05 (s), 129.30 (s), 129.29 (t, $J_{PC} = 5.4$ Hz, PPh₃), 128.9 (s), 128.4 (s), 128.2 (s), 126.8 (t, $J_{PC} = 27$ Hz, *ipso*-PPh₃), 111.6 (t, $J_{PC} = 6$ Hz, Ir-C), 32.3 (s), 24.8 (s). ³¹P{¹H} NMR (161.9 MHz, CD₂Cl₂, 298 K): δ 6.48 (s). Anal. Calcd for C₅₆H₄₈BF₄IrO₂P₂: C, 61.48; H, 4.42. Found: C, 61.73; H, 4.49.

The synthesis of **18b** (SbF₆⁻) is also directly analogous to that of **17** using **1** (SbF₆⁻, 85 mg, 0.073 mmol) and Ph-C≡C(O)OEt (25 mg, 0.144 mmol). Yield: 88% (82 mg, 0.065 mmol). ¹H NMR (500 MHz, CD₂Cl₂, 295 K): δ 7.30–7.55 (m, 31H), 7.27 (t, $^3J_{HH} = 7.6$ Hz, 2H), 7.15–7.25 (m, 3H), 7.03 (d, $^3J_{HH} = 7.6$ Hz, 2H), 6.70 (d, $^3J_{HH} = 7.9$ Hz, 2H), 6.58 (s, 1H), 6.29 (s, 1H), 3.22 (q, $^3J_{HH} = 7.2$ Hz, 2H), 1.50 (s, 3H), 0.65 (t, $^3J_{HH} = 7.2$ Hz, 3H). ¹³C NMR (125 MHz, CD₂Cl₂, 295 K): δ 212.7 (s), 197.7 (t, $J_{PC} = 5.4$ Hz, iridafuran Ir-C), 184.7 (s), 147.7 (s), 145.4 (s), 138.8 (s), 137.6 (s), 135.5 (t, $J_{PC} = 5.4$ Hz, PPh₃), 132.2 (s), 131.0 (s), 129.2 (t, $J_{PC} = 5.4$ Hz, PPh₃), 129.1 (s), 128.6 (s), 128.4 (s), 128.2 (s), 126.3 (t, $J_{PC} = 26.9$ Hz, *ipso*-PPh₃), 104.0 (t, $J_{PC} = 7.5$ Hz, Ir-C), 63.4 (s), 24.5 (s), 13.6 (s). ³¹P{¹H} NMR (161.9 MHz, CD₂Cl₂, 298 K): δ 5.54 (s). Anal. Calcd for C₅₇H₅₀F₆IrO₃P₂Sb·CH₂Cl₂: C, 51.30; H, 3.86; Cl, 5.22. Found: C, 51.33; H, 3.84; Cl, 5.57.

trans-Bis(triphenylphosphine)(η^2 -{O,C1}-1-phenylbut-1-en-3-on-1-yl)(carbonyl)(ethylbut-2-(E)-enoat-2-yl)iridium(III) Hexafluoroantimonate [19 (SbF₆⁻)]. The complex **18b** (SbF₆⁻, 30 mg, 0.024 mmol) was dissolved in CH₂Cl₂ (6 mL), and CO (1 atm) was bubbled through the solution for 1 h. Diethyl ether (15 mL) was then added to this solution to give a light yellow precipitate, which was filtered, washed with diethyl ether (2 × 10 mL), and dried in vacuo. Yield: 30 mg (0.023 mmol, 99%). ¹H NMR (500 MHz, CD₂Cl₂, 295 K): δ 7.32–7.60 (m, 33H), 7.20 (t, $^3J_{HH} = 7.6$ Hz, 2H), 7.10–7.15 (m, 3H), 6.84 (s, 1H), 6.30–6.35 (m, 2H), 5.73 (s, 1H), 3.66 (q, $^3J_{HH} = 7.2$ Hz, 2H), 1.52 (s, 3H), 0.76 (t, $^3J_{HH} = 7.2$ Hz, 3H). ¹³C NMR (125 MHz, CD₂Cl₂, 295 K): δ 219.1 (t, $J_{PC} = 9.0$ Hz, iridafuran Ir-C), 215.8 (s), 176.2 (s), 172.5 (t, $J_{PC} = 8.6$ Hz, Ir-CO), 151.4 (s), 143.9 (s), 143.4 (s), 140.1 (s), 135.7 (t, $J_{PC} = 5.8$ Hz, PPh₃), 132.8 (s), 132.0 (s), 131.4 (s), 129.4 (t, $J_{PC} = 5.8$ Hz, PPh₃), 128.4 (s), 128.2 (s), 127.6 (t, $J_{PC} = 27.8$ Hz, *ipso*-PPh₃), 127.5 (s), 107.1 (t, $J_{PC} = 7.0$ Hz, Ir-C), 61.9 (s), 25.8 (s), 13.7 (s). ³¹P{¹H} NMR (161.9 MHz, CD₂Cl₂, 298 K): δ -7.4 (s) IR (cm⁻¹): 2063 (ν_{CO} , IrCO), 1679 (ν_{CO} , ester). Anal. Calcd for C₅₈H₅₀F₆IrO₄P₂Sb: C, 53.55; H, 3.87. Found: C, 53.47; H, 4.12.

Structure Determination of 12a·acetone, 15a, and 18a·Et₂O. Crystals of **12a** was obtained by layering its acetone solution with pentane. Crystals of **15a** and **18a** were obtained by slow diffusion of Et₂O into their CH₂Cl₂ solutions. Suitable crystals were selected and mounted on thin glass fibers using epoxy cement and cooled to data collection temperature. All measurements were made on a Nonius KappaCCD diffractometer with graphite-monochromated Mo K α radiation, and intensity data were collected by using the ω -scan mode. The data were corrected for Lorentz and polarization effects, and no absorption correction was applied. The structures were solved by direct methods and refined by full-matrix least-

squares techniques. The non-hydrogen atoms were refined anisotropically, and hydrogen atoms were treated as idealized contributions.

Complex **12a** cocrystallized with one molecule of acetone that possesses a high degree of thermal motion. To counter the effect of inflated thermal parameters, the carbon–carbon and carbon–oxygen bonds were fixed at ideal lengths and non-hydrogen atoms were refined isotropically.

Complex **15a** crystallized in the *C*-centered monoclinic space group *C*2 with one molecule in the asymmetric unit and four molecules in the unit cell. In the asymmetric unit, the hexafluorantimonate counterion resides on a 2-fold axis of rotation, resulting in two crystallographically independent $\text{Sb}_{0.5}\text{F}_3$ fragments. While one fragment is well ordered, the second is plagued with positional disorder. Alternative sites (50:50) were modeled for each of the fluorine atoms, and both components of the disorder were refined with anisotropic displacement parameters.

Complex **18a** cocrystallized with diethyl ether in a ratio of 1:1. Squeeze/Platon²⁵ was applied to resolve one molecule of severely disordered diethyl ether within the asymmetric unit.

(25) Spek, A. L. *Acta Crystallogr.* **1990**, *A46*, C34.

Within the 245.5 Å³ unit cell void space occupied by solvent molecules, a total of 84 electrons were calculated, compared to 84 electrons for the two molecules of solvent. In this treatment of solvent, the contributions of the solvent molecules are collective and not as individual atoms. Hence, the atom list (see Supporting Information) does not contain the atoms of the solvent molecules. For **18a**, the BF_4^- counterion is plagued with positional disorder. Alternative sites for F(2–4) were effectively modeled with occupancy factor ratios of 50:50. All boron and fluorine atoms were refined with anisotropic displacement parameters, and the B–F bonds were restrained to ideal distances for ease of refinement.

Acknowledgment. Generous financial support from the U.S. Department of Energy and the Johnson Matthey Company is greatly acknowledged.

Supporting Information Available: Detailed X-ray crystallographic data of atomic positional parameters, bond distances and angles, and anisotropic thermal parameters (PDF and CIF) for **12a**, **15a**, and **18a**. This material is available free of charge via the Internet at <http://pubs.acs.org>.

OM049271Z